Original Research

Gas chromatography-mass spectrometry metabolic profiling, molecular simulation and dynamics of diverse phytochemicals of *Punica granatum* L. leaves against estrogen receptor

Talambedu Usha[1], Sushil Kumar Middha[2,*], Dhivya Shanmugarajan[2], Dinesh Babu[3], Arvind Kumar Goyal[4], Hasan Soliman Yusufoglu[5], Kora Rudraiah Sidhalinghamurthy[1]

[1]*Department of Biochemistry, Bangalore University, Bengaluru, 560029 Karnataka, India,* [2]*DBT-BIF Facility, Department of Biotechnology, Maharani Lakshmi Ammanni College for Women, 560012 Bangalore, India,* [3]*Faculty of Pharmacy and Pharmaceutical Sciences, University of Alberta, Edmonton, AB T6G 2E1, Canada,* [4]*Centre for Bamboo Studies, Department of Biotechnology, Bodoland University, Kokrajhar, 783370 Assam, India,* [5]*College of Pharmacy, Prince Sattam Bin Abdulaziz University, 16278 Al-Kharj, Saudi Arabia*

TABLE OF CONTENTS

1. Abstract

Introduction: Breast cancer is the most common type of cancer globally and its treatment with many FDA-approved synthetic drugs manifests various side effects. Alternatively, phytochemicals are natural reserves of novel drugs for cancer therapy. *Punica granatum* commonly known as pomegranate is a rich source of phytopharmaceuticals. **Methods**: The phytoconstituents of *Punica granatum* leaves were profiled using GC-MS/MS in the present work. Cytoscape-assisted network pharmacology of principal and prognostic biomarkers, which are immunohistochemically tested in breast cancer tissue, was carried out for the identification of protein target. Followed by, rigorous virtual screening of 145 phytoconstituents against the three ER isoforms (α, β and γ) was performed using Discovery Studio. The docked complexes were further evaluated for their flexibility and stability using GROMACS2016 through 50 ns long molecular dynamic simulations. **Results:** In the current study, we report the precise and systematic GC-MS/MS profiling of phytoconstituents (19 novel metabolites out of 145) of hydromethanolic extract of *Punica granatum* L. (pomegranate) leaves. These phytocompounds are various types of fatty acids, terpenes, heterocyclic compounds and flavonoids. 4-coumaric acid methyl ester was identified as the best inhibitor of ER isoforms with drug-likeness and no toxicity from ADMET screening. γ-ligand binding domain complex showed the

Submitted: 14 January 2021 Accepted: 19 March 2021 Published: 30 September 2021
This is an open access article under the CC BY 4.0 license (https://creativecommons.org/licenses/by/4.0/).
© 2021 The Author(s). Published by BRI.

best interactions with minimum RMSD, constant Rg, and the maximum number of hydrogen bonds. **Conclusion**: We conclude that 4-coumaric acid methyl ester exhibits favourable drug-like properties comparable to tamoxifen, an FDA-approved breast cancer drug and can be tested further in preclinical studies.

2. Introduction

Drug discovery is a multifaceted and interdisciplinary endeavor that pursues a sequential process, begins with the discovery of a target and lead, followed by lead optimization and preclinical studies to define and verify the suitability of such lead agents through a number of predetermined guidelines for kick-starting clinical development [1, 2]. The high cost and time-consuming nature of these processes against an ailment demand a novel kind of cost-effective and less time-consuming, intensive *in-silico* approach [2, 3]. *In-silico* techniques employ bioinformatics tools to identify drug targets, to explore target protein structure for prediction of possible active sites to dock molecules with targets, rank ligands based on their binding affinities (i.e., energies), and optimize lead molecules [4]. Proficiency in calculating precise, significant, and diverse conformations of ligands within the target site make the molecular docking the most desired drug designing tool [5]. Hence, this tool can be used to understand the various interactions between phytochemicals and breast cancer targets or biomarkers. Despite the availability of modern tools and increasing expertise to identify a new anticancer molecule or lead, the potential of natural products (medicinal plants) and their compounds remains immense and undiscovered.

Many FDA-approved drugs such as paclitaxel and vinblastine (anticancer drugs), and quinine and artemisinin (antimalarial drugs) are plant-based. Therefore, combining the potential of phytomedicine with modern technology can help to develop more effective and economical drugs [6]. Phytochemicals from medicinal plants not only serve as drugs but also provide a lead for the development of new drugs. *Punica granatum* L., commonly known as pomegranate, is one such medicinal plant with a known reservoir of active biomolecules such as a series of compounds known as ellagitannins, and specifically punicalagin, the unique largest molecular weight polyphenol known to date [7]. A plethora of research reports describe the vasculo protective [8], antidiabetic, antioxidant [7], antiproliferative [9], antitumor [9, 10], anti-inflammatory [11], neuroprotective [12], and antimicrobial [13] properties of pomegranate along with its potential for treating asthma [14]. Previously, Usha *et al*. (2014) [15] have identified anticancer targets from pomegranate using an *in-silico* approach.

Breast cancer is the most common type of cancer worldwide, which affects 2.1 million women annually. In the year 2018, the World Health Organization estimated that 627,000 deaths in women were caused due to breast cancer accounting for nearly 15% of all cancer-related mortality among women (https://www.who.int/cancer/detection/breastcancer/en/) [16]. The current study aims at identifying a lead molecule for breast cancer from a natural source like pomegranate. Aromatase is an enzyme that converts C19 androgen to C18 estrogen that plays a vital role in breast cancer, which was reported to be present in high concentrations in breast tumors [17]. Several ellagitannins-derived compounds isolated from pomegranate were previously reported to have potential anti-aromatase activity and inhibit testosterone-induced breast cancer cell proliferation [18]. However, there is a dearth of knowledge about the molecular basis and mechanism(s) of these compounds against breast cancer. The aim of the present study is to design a drug-like entity for breast cancer from *Punica granatum* L. phytochemicals. To be specific, our study involves a gas chromatography-mass spectrometry (GC-MS)/MS-based metabolite profiling of hydromethanolic extract of *Punica granatum* L. leaves (HMPGL), to identify a lead candidate, which can act as an antagonist and further verification against the ligand-binding domains (LBDs) of the three different isoforms of human estrogen receptor (ER), namely, ER alpha (ERα), ER beta (ERβ) and estrogen-related receptor (ERR) gamma (ERRγ) using molecular dynamics approach. Our finding reveals that 2-propenoic acid, 3-(4-hydroxyphenyl)-, methyl ester alias 4-coumaric acid methyl ester could act as an antagonist for LBDs of ERα, ERβ and ERRγ isoforms of ER, suggesting its future potential for the development of breast cancer therapeutics.

3. Materials and methods

3.1 *In-vitro* analyses

3.1.1 Collection of plants and preparation of crude extract

The leaves of *Punica granatum* L. plant were collected from Gandhi Krishi Vignan Kendra (GKVK), Bengaluru, Karnataka, India. After authentication by the plant taxonomist, a voucher specimen (BOT/mLAC/BMPG001) has been submitted to Botany Department, Maharani Lakshmi Ammanni College for Women, Bengaluru, Karnataka, India. The leaves were shade dried, grounded, and the powder was subjected to soxhlation using 70% methanol as a solvent system. The extract was lyophilized using freeze-drying technology under –55 °C and at constant pressure. The extract thus obtained was used further for analysis.

3.1.2 Determination of hydromethanolic leaf extract yield

The yield of hydromethanolic leaf extract was calculated using the following equation: Yield (g/100 g of dry plant material) = (W1 $\times$ 100) / W2, where W1-weight of the extract after solvent evaporation and W2-weight of dry plant material (leaves).

Table 1. List of 145 phytocompounds identified in the hydromethanolic extract of *Punica granatum* L. leaves by GC-MS/MS. * is used for novel compounds identified (19 metabolites).

S. No	Retention time	Compound name	Chemical formula	Area	MW (g/mol)
1	11.6496	(3-Nitrophenyl) methanol, n-propyl ether	$C_{10}H_{13}NO_3$	728600034	195.21
2	12.1305	(4H)4a,5,6,7,8,8a-Hexahydrobenzopyran-5-one-3-carboxamide,2-(2-hydroxypentyl)-8a-methoxy-4a-methyl	$C_{17}H_{27}NO_5$	28662212	325.40
3	24.6876	Alpha-Tocospiro A	$C_{29}H_{50}O_4$	1087514521	462.70
4	24.8403	Alpha-Tocospiro B	$C_{29}H_{50}O_4$	909893093	462.00
5	25.9167	Gamma-Tocopherol	$C_{28}H_{48}O_2$	77931713	416.70
6	6.9628	[1,2,3,4]Tetrazolo[1,5-b][1,2,4]triazine,5,6,7,8-tetrahydro-	$C_3H_6N_6$	1406037645	126.12
7	12.5427	1,1,4,5,6-Pentamethyl-2,3-dihydro-1H-indene	$C_{14}H_{20}$	470619079	188.31
8	11.4893	1,2,3,6-Tetrahydropyridine, 1-methyl-5-phenyl-	$C_{12}H_{15}N$	2272849467	173.25
9	10.9855	1,2,3-Benzenetriol	$C_6H_6O_3$	29449616456	126.11
10*	9.8863	1,8-Dioxaspiro[4.5]decan-2-one, 4-(2-aminothiazol-4-yl)-7,7-dimethyl-	$C_{13}H_{18}N_2O_3S$	392180530	282.00
11*	3.3827	1H-Cyclopropa[3,4]benz[1,2-e]azulene- 4a,5,7b,9,9a(1aH)-pentol, 3-[(acetyloxy)methyl]-1b,4,5,7a,8a9-hexahydro-1,1,6,8-tetramethyl-,5,9,9a-triacetate, [1aR-(1a.alpha., 1b.beta.,4a.beta.,5.beta.,7a.alpha.,7b.alpha.,8.alpha.,9.beta.,9a.alpha)	$C_{28}H_{38}O_{10}$	50122079	534.59
12	8.3139	1H-Imidazole, 1-methyl-	$C_4H_6N_2$	58733639	82.10
13	12.9549	1H-Inden-1-one, 2,3-dihydro-3,3,4,6-tetramethyl-	$C_{13}H_{16}O$	920997462	188.26
14	11.7031	1H-Inden-1-one, 2,3-dihydro-3,3,5,6-tetramethyl	$C_{13}H_{16}O$	548026939	188.26
15	16.1457	2-(3-Isopropyl-4-methyl-pent-3-en-1-ynyl)-2-methyl-cyclobutanone	$C_{14}H_{20}O$	383367099	204.31
16*	12.8862	2-(3-Isopropyl-4-methyl-pent-3-en-1-ynyl)-2-methyl-pent-3-en-1-ynyl-2-methylcyclobutanone	$C_{14}H_{20}O$	264669072	204.00
17	12.8328	2(4H)-Benzofuranone, 5,6,7,7a-tetrahydro-4,4,7a-trimethyl-,(R)-	$C_{11}H_{16}O_2$	828417676	180.24
18	3.5354 4.4285	2(5H)-Furanone	$C_4H_4O_2$	532754993 287429887	84.07
19	3.3140	2,2'-Bioxirane	$C_4H_6O_2$	455025294	86.09
20	6.4666	2,4(1H,3H)-Pyrimidinedione, 5-hydroxy-	$C_4H_4N_2O_3$	90374515	128.09
21*	2.7949	2,4,6,8,10-Tetradecapentaenoic acid, 9a-decahydro-4a,7b-dihydroxy-3-(hydroxymethyl)-cyclopropa[3,4]benz[1,2-e]azulen-9-yl ester, (1a.alpha.,1b.beta.,4a.beta.,7a.alpha.,7b.alpha, 8.alpha, 9.beta,9a.alpha.)	$C_{36}H_{46}O_8$	1729589562	606.00
22	5.1842	2,4-Dihydroxy-2,5-dimethyl-3(2H)-furan-3-one	$C_6H_8O_4$	1800447816	144.12
23	12.474	2,4-Di-tert-butylphenol	$C_{14}H_{22}O$	162473760	206.32
24	13.1534	2,5-Dimethoxy-4-ethylamphetamine	$C_{13}H_{21}NO_2$	258752481	223.31
25	6.6040	2,5-Furandicarboxaldehyde	$C_6H_4O_3$	194264167	124.09
26*	3.0926	2-[4-Chloro-2-nitrophenyl]-1-(2-diethyaminoethyl)-3-formyl-1H-indole	$C_{21}H_{22}ClNO_3$	55662163	399
27	4.5201	2-Amino-4-methyl-oxazole	$C_4H_6N_2O$	518087636	98.10
28	14.1915	2-Cyclohexen-1-one, 4-(3-hydroxy-1-butenyl)-3,5,5-trimethyl-	$C_{13}H_{20}O_2$	560078241	208.30
29	15.6113	2-Dodecen-1-yl(-)succinic anhydride	$C_{16}H_{26}O_3$	133093417	266.38
30	4.9781	2-Furancarboxaldehyde, 5-methyl-	$C_6H_6O_2$	898805469	110.11
31	6.9017	2-Furancarboxylic acid	$C_5H_4O_3$	661021535	112.08
32	3.9018	2-Furanmethanol	$C_5H_6O_2$	2300435655	98.10
33	6.1460	2-Heptanol, 5-ethyl-	$C_9H_{20}O$	358696294	144.25
34	4.7873	2-Hexene, 4-methyl-, (E)-	C_7H_{14}	92798753	98.19
35	9.3062	2H-Pyran, 2-(bromomethyl)tetrahydro-	$C_6H_{11}BrO$	39730800	179.05
36	5.4056	2H-Pyran-2,6(3H)-dione	$C_5H_4O_3$	511684838	112.08
37	6.3674	2-Methylthio-2,3-dimethylbutane	$C_7H_{16}S$	191303503	132.27
38	15.0541	2-Propanone, 1-hydroxy-3-(4-hydroxy-3-methoxyphenyl)-	$C_{10}H_{12}O_4$	76991990	196.20
39	15.2297	2-Propenoic acid, 3-(4-hydroxyphenyl)-, methyl ester or 4- Coumaric acid methyl ester	$C_{10}H_{10}O_3$	79623370	178.18

Table 1. Continued.

S. No	Retention time	Compound name	Chemical formula	Area	MW (g/mol)
40	11.7489	3,3-Dimethyl-4-phenyl-4-penten-2-one	$C_{13}H_{16}O$	815120462	188.26
41	13.2984	3a,7-Methano-3aH-cyclopentacyclooctene, decahyydro-1,1,7-trimethyl-,[3aS-(3a.alpha.,7.alpha.,9a.beta.)]-	$C_{15}H_{26}$	99198977	191.00
42	8.1918	3-Amino-N-(pyridin-4-yl)propanamide	$C_8H_{11}N_3O$	46243181	165.19
43*	4.8789	3-Aminopyrazine 1-oxide	$C_4H_5\ N_3O$	69030002	111.00
44	14.5503	3-Chloropropionic acid, heptadecyl ester	$C_{20}H_{39}ClO_2$	971108451	347.00
45	3.7338 6.6804	3-Furaldehyde	$C_5H_4O_2$	2958433873 1614869390	96.08
46	3.6422	3-Furanmethanol	$C_5H_6O_2$	505585085	98.10
47	14.8327	3-Furoic acid, benzyldimethylsilyl ester	$C_{14}H_{16}O_3Si$	203867247	260.36
48	15.9319	3H-Cyclodeca[b]furan-2-one, 4,9-dihydroxy-6-methyl-3,10,dimethylene-3a,4,7,8,9,10,11,11a-octahydro-	$C_{15}H_{20}O_4$	257866769	264.32
49	16.1075	3-Hexadecyne	$C_{16}H_{30}$	586051279	222.41
50	16.3670	3-Octadecyne	$C_{18}H_{34}$	162514947	250.50
51	12.1840	4-(2,6,6-Trimethylcyclohexa-1,3-dienyl)but-3-en-2-one	$C_{13}H_{18}O$	19815134	190.28
52	14.2984	4,4,5,8-Tetramethylchroman-2-ol	$C_{13}H_{18}O_2$	1110933501	206.28
53	7.7261	4H-Pyran-4-one, 2,3-dihydro-3,5-dihydroxy-6-methyl-	$C_6H_8O_4$	7618503933	144.12
54	8.2757	4H-Pyran-4-one, 3,5-dihydroxy-2-methyl-	$C_6H_6O_4$	434272719	142.11
55	7.4284	4H-Pyran-4-one, 5-hydroxy-2-methyl-	$C_6H_6O_3$	802533562	126.11
56	9.9627	4-Hydroxy-2-methylacetophenone	$C_9H_{10}O_2$	1075532343	150.17
57	17.8479	5-(2-Morpholino-1-thiophen-2-yl-vinyl)-1,2,4-thiadiazole	$C_{12}H_{13}N_3OS_2$	39520603	279.40
58	15.7335	5,5,8a-Trimethyl-3,5,6,7,8,8a-hexahydro-2H-chromene	$C_{12}H_{20}O$	458070336	180.29
59*	25.39	5H-Cyclopropa[3,4]benz[1,2-e]azulen-5-one, chloro-1,1a,1b,2,3,4,4a,7a,7b,8,9,9a- tetramethyl-, [1aR-(1a.aplha.,7b.alpha.,8.alpha.9.beta.,9a.alpha)]	$C_{28}H_{37}ClO_{11}$	53025185	489
60*	18.4891	5H-Cyclopropa[3,4]benz[1,2-e]azulen-5-one,9,9a-bis(acetyloxy)-3-[(acetoxy)methyl]-1,1a,1b,2,3,4,4a,7a,7b,8,9,9a-dodecahydro-2,3,4a,7b-tetrahydroxy-1,,6,8-tetramethyl-,[1ar-(1a.alpha.,1b.beya,2.alpha.,3.alpha.,4a.beta.,7a.alpha.,7b.alpha.,8.alpha.,9.beta.,9a.alpha)	$C_{26}H_{36}O_{11}$	62085503	446.00
61	9.0390	5-Hydroxymethylfurfural	$C_6H_6O_3$	12338767206	126.11
62	13.6572	5-Isopropenyl-2-methylcyclopent-1-enecarboxaldehyde	$C_{10}H_{14}O$	344352899	150.22
63	15.5197	6-Hydroxy-4,4,7a-trimethyl-5,6,7,7a-tetrahydrobenzofuran-2(4H)-one	$C_{11}H_{16}O_3$	607605365	196.24
64	18.4128	7,8,9,10-Tetrahydro-6(5H)-phenanthridinone	$C_{13}H_{13}NO$	83259442	199.25
65	25.8709	7,8-Epoxylanostan-11-ol, 3-acetoxy-	$C_{32}H_{54}O_4$	53150204	502.80
66	16.5502	7-Heptadecyne, 17-chloro-	$C_{17}H_{31}Cl$	206699451	270.90
67	20.5654	8,11,14-Eicosatrienoic acid, methyl ester,(Z,Z,Z)-	$C_{21}H_{36}O_2$	114885329	320.50
68	19.1532	9,12,15-Octadecatrienoic acid, (Z,Z,Z)-	$C_{18}H_{30}O_2$	30390789406	278.40
69	16.4739 23.5395	9,12,15-Octadecatrienoic acid, 2,3-dihydroxypropyl, ester (Z,Z,Z)-	$C_{21}H_{36}O_4$	80048369 2227344617	352.50
70	22.5120	9,12,15-Octadecatrienoic acid, ethyl ester, (Z,Z,Z)-	$C_{20}H_{34}O_2$	364409437	306.50
71	18.6799	9,12,15-Octadecatrienoic acid, methyl ester,(Z,Z,Z)	$C_{19}H_{32}O_2$	5071324434	292
72	18.6112	9,12-Octadecadienoic acid (Z,Z)-, methyl ester	$C_{19}H_{34}O_2$	2018420993	294.50
73	18.0922	9-Hexadecenoic acid	$C_{16}H_{30}O_2$	510568704	254.41
74*	23.2907	Acetic acid, 17-acetoxy-3-hydroxyimino-4,4,13-hexadecahydrocyclopenta[a]phenanthren-10-ylmetyl ester	$C_{25}H_{39}ONO_5$	90416430	433.00
75	11.3290	Azetidine, 1,1’-methylenebis[2-methyl-	$C_9H_{18}N_2$	4498160447	154.25
76	11.9550	Benzaldehyde, 4-ethyl-	$C_9H_{10}O$	327861429	134.17
77	8.6345	Benzofuran, 2,3-dihydro-	C_8H_8O	2678521082	120.15
78	16.7869	Benzoic acid, 3,4,5-trihydroxy-, methyl ester	$C_8H_8O_5$	168553503	184.15
79	12.6649	Benzoic acid, 4-ethoxy-, ethyl ester	$C_{11}H_{14}O_3$	183455032	194.23
80	9.3749	Benzoic acid, 4-methyl-	$C_8H_8O_2$	28589154	136.15
81	5.9705	Benzyl alcohol	C_7H_8O	821031061	108.14
82	7.9857	beta.-1,5-Dibenzoyl-2-deoxy-ribofuranose	$C_{19}H_{18}O_6$	372597103	342.3
83	13.8251	Bicyclo[2.2.1]hept-2-ene, 1,7,7-trimethyl-	$C_{10}H_{16}$	275857190	136.23

Table 1. Continued.

S. No	Retention time	Compound name	Chemical formula	Area	MW (g/mol)
84	4.1384	But-1-ene-3-yne, 1-ethoxy-	C_6H_8O	568495293	96.13
85	13.4358	Butyrovanillone	$C_{11}H_{14}O_3$	22430637	194.22
86*	24.2296/25.5884	Carbonic acid, eicosyl vinyl ester	$C_{23}H_{44}O_3$	702086983/ 675042558	368.60
87	8.436	Catechol	$C_6H_6O_2$	104187122	110.11
88	23.3517	cis-5,8,11,14-Eicosatetraenoic acid, picolinyl ester	$C_{26}H_{37}NO_2$	75303340	395.60
89*	8.52	Cyclobutane, 1,2:3,4-di-O-ethylboranediyl-	$C_8H_{14}B_2O_4$	117519035	195.82
90	5.5735	Cyclohexane, 1,3,5-trimethyl-2-octadecyl-	$C_{27}H_{54}$	43383586	126.10
91*	16.1762	Cyclopropane, 1 heptaonyl-3-methylene-2-pentyl-	$C_{16}H_{28}O$	301623110	378.7
92*	17.138	Cyclopropanepctanoic acid, 2-[(-pentylcyclopropyl)methyl]-,methyl ester, trans, trans-	$C_{12}H_{13}N_3OS_2$	39520603	322.00
93*	5.7644	Cyclopropylamine, N-isobutylidene-	$C_7H_{13}N$	133377747	111.18
94*	13.0465	Dihydroxanthin	$C_{17}H_{24}O_5$	492844334	280.00
95	14.0846	Doconexent	$C_{22}H_{32}O_2$	146857459	328.5
96*	21.2677	Doconexent, TBDMS derivative	$C_{28}H_{46}O_2Si$	31973570	442.70
97	11.9931	E-11,13-Tetradecadien-1-ol	$C_{14}H_{26}O$	430872421	210.36
98	20.9319	Eicosanoic acid	$C_{20}H_{40}O_2$	795269485	312.50
99	4.3827	Ethanone, 1-(2-furanyl)-	$C_6H_6O_2$	165889275	110.11
100	20.3364	Ethyl 5,8,11,14,17-icosapentaenoate	$C_{22}H_{34}O_2$	252266022	330.50
101*	24.5731/ 24.7945	Furan, 2,5-bis(3,4-dimethoxyphenyl)tetrahydro-3,4-dimethyl-,[2R-(2.alpha.,3.beta.,4.beta.,5.alpha.)]	$C_{22}H_{28}O_5$	101227511/ 485260974	372.00
102	4.3064	Furan-2-ylmethyl palmitate	$C_{21}H_{36}O_3$	36491320	336.50
103	21.4662	Heneicosanoic acid, methyl ester	$C_{22}H_{44}O_2$	34798280	340.60
104	22.0158/22.7792	Heptacosane	$C_{27}H_{56}$	291521130/ 296780030	380.70
105	22.199	Hexadecanoic acid, 1-(hydroxymethyl)-1,2-ethanediyl ester	$C_{35}H_{68}O_5$	317213707	568.90
106	17.9624	Hexadecanoic acid, 15-methyl-, methyl ester	$C_{18}H_{36}O_2$	82387516	284.50
107*	22.1151	Hexadecanoic acid, 2-hydroxy-1-(hydroxymethyl)ethyl ester	$C_{19}H_{38}O_4$	2065095285	330.00
108	16.9853	Hexadecanoic acid, methyl ester	$C_{17}H_{34}O_2$	3020358912	270.50
109	19.9395	Indane-4-carbonitrile, 2,2,5,7-tetramethyl-1-oxo	$C_{14}H_{15}NO$	71510002	213.27
110	9.7108	Indole	C_8H_7N	20622699	117.15
111	22.9395	Licarin A	$C_{20}H_{22}O_4$	224689115	326.40
112	7.2223	Maltol	$C_6H_6O_3$	14939408876	126.11
113	15.3671	Mannofuranoside, 1-allyl-2,3-5,6-tetra-O-acetyl-	$C_{17}H_{24}O_9$	25787993	372.40
114	13.7717	Megastigmatrienone	$C_{13}H_{18}O$	240529958	190.00
115*	16.0617	Methanone, (2,6-dimethyl-4-morpholyl)(9H-xanthen-9-yl)-	$C_{20}H_{21}NO_3$	238398621	323.40
116	5.3293	Methanone, [4-(2-furfurylthio)-3-nitrophenyl](morpholino)	$C_{16}H_{16}N_2O_5S$	76240602	348.40
117	23.7487	Methyl 18-methylicosanoate	$C_{22}H_{44}O_2$	148572467	340.60
118	20.6418	Methyl 18-methylnonadecanoate	$C_{21}H_{42}O_2$	237808761	326.60
119	18.8937/22.2525	Methyl stearate	$C_{19}H_{38}O_2$	831716164/ 166816879	298.50
120	5.459	N-Butyl-tert-butylamine	$C_8H_{19}N$	514116590	129.24
121	17.451	n-Hexadecanoic acid	$C_{16}H_{32}O_2$	16562951600	256.42
122	16.6266	Nootkaton-11,12-epoxide	$C_{15}H_{22}O_2$	174277673	234.33
123	17.6418/21.0769	Octadecanal, 2-bromo-	$C_{18}H_{35}BrO$	305383125/ 46483241	347.4
124	21.2143	Octadecane, 3-ethyl-5-(2-ethylbutyl)-	$C_{26}H_{54}$	94740807	364.00
125	5.8789/21.909	Octadecanedioic acid	$C_{18}H_{34}O_4$	34874865/ 234355861	314.5
126	19.283	Octadecanoic acid	$C_{18}H_{36}O_2$	3813012247	284.5
127	23.6647	Octadecanoic acid, 2,3-dihydroxypropyl ester	$C_{21}H_{42}O_4$	433327098	358.6
128	20.4357	Oxiranedodecanoic acid, 3-octyl-, cis-	$C_{22}H_{42}O_3$	15785811	354.6
129	22.4357	Phthalic acid, octyl tridec-2-yn-1-yl ester	$C_{29}H_{44}O_4$	486477919	456.7

Table 1. Continued.

S. No	Retention time	Compound name	Chemical formula	Area	MW (g/mol)
130	18.7792	Phytol	$C_{20}H_{40}O$	776137812	296.50
131	20.7563	Pregnane-7,8,9,11,20-pentaol-18-oic acid,7,11-diacetate-18,20-lactone	$C_{25}H_{34}O_9$	49740067	478.50
132	3.2224	Propane, 2-fluoro-	C_3H_7F	193906460	62.09
133	6.5506	Pyridazine	$C_4H_4N_2$	251310771	80.09
134	24.4739	Squalene	$C_{30}H_{50}$	923530021	410.70
135	24.9167	Sulfurous acid, hexyl pentadecyl ester	$C_{21}H_{44}O_3S$	1241617690	376.60
136	13.9091/13.3595	syn-Tricyclo[5.1.0.0(2,4)]oct-5-ene, 3,3,5,6,8,8-hexamethyl-	$C_{14}H_{22}$	1025801501/ 321999626	190.32
137	15.2831/18.2906	Tetradecanoic acid	$C_{14}H_{28}O_2$	324806663/ 394717404	228.37
138	20.0234	Tetradecanoic acid, 2-hydroxy-	$C_{14}H_{28}O_3$	269881507	244.37
139	6.833	Thymine	$C_5H_6N_2O_2$	1117152651	126.11
140	14.6419	Tibolone	$C_{21}H_{28}O_2$	783232577	312.40
141	3.0621	Trifluoromethyltrimethylsilane	$C_4H_9F_3Si$	112646880	142.19
142	16.3136	Undecanoic acid, 2-nonyl-, methyl ester	$C_{21}H_{42}O_2$	109936717	326.60
143	10.4588	Undecanol-5	$C_{11}H_{24}O$	5922534581	172.31
144	20.2067/21.6494	Ursodeoxycholic acid	$C_{24}H_{40}O_4$	34678472/ 97533782	396.60
145	20.0845	Z-(13,14-Epoxy)tetradec-11-en-1-ol acetate	$C_{16}H_{28}O_3$	320849197	268.39

3.1.3 Preliminary screening of phytochemicals in hydromethanolic extract of *Punica granatum* L. leaves (HMPGL)

Qualitative phytochemical analysis of HMPGL, for the detection of alkaloids, carbohydrates, flavonoids, glycosides, phenols, saponins, steroids, tannins [19], fatty acids, coumarins and resins [20] was carried out as per the standard procedures.

3.1.4 1,1-diphenyl-2-picrylhydrazyl (DPPH) radical scavenging activity

DPPH radical scavenging assay was used to determine the antioxidant activity of HMPGL. Sample aliquots of different concentrations were incubated with 1.8 mL of DPPH for 30 min at room temperature and the absorbance was measured at 540 nm [19]. The ability of the HMPGL to scavenge DPPH radical was calculated using the standard formula: DPPH free radical scavenging activity (%) = (Absorbance of control (DPPH)–Absorbance of DPPH radical + HMPGL)/(Absorbance of control (DPPH)) $\times$ 100.

3.1.5 Total phenolic content

The total phenolic content of HMPGL was estimated using the Folin-Ciocalteu reagent as previously reported by Goyal *et al.* 2010 [19].

3.1.6 Phytoconstituent profiling of hydromethonolic extract by GC-MS/MS analysis

The gas chromatogram-mass spectrometer (Agilent Technologies 7890B GC and Triple Quadrupole mass spectrometer 7000D series) was used for the analysis, having a blend silica column, bundled with 5% biphenyl 95% dimethylpolysiloxane (Elite-5MS), merged with a capillary column (30 m $\times$ 0.25 mm $\times$ 1 μm). Helium quench gas and nitrogen collision gas were deployed as a carrier gas at a regular flow rate of 2.25 mL/min and 1.5 mL/min, respectively, and a pressure of 8.745 psi to separate different components found in the test sample. Each chromatographic run was adjusted at 260 °C injector temperature. 2 μL volume of the 100$\times$ diluted sample was injected in the instrument (a split ratio of 10 : 1). The oven temperature was in the range of 20 °C to 260 °C. The mass detector conditions were as follows: transfer line temperature 300 °C; ion source temperature 260 °C; ionization mode electron impact at 70 eV, a scan time 0.2 sec and scan interval of 0.1 sec. The sample was analyzed within a mass range of 50 *m/z* to 1000 *m/z*. The solvent delay was 0 to 2 min, and the total GC-MS/MS running time was 44 min. The mass spectrum of each peak in the total ion chromatogram was compared with the databases of The National Institute of Standards and Technology (NIST) 14 MS Library containing '276248' number of compound's spectral databases. The IUPAC names, molecular formulae, molecular weights, and structure of the metabolites of HMPGL were thereby ascertained.

3.2 Computational analysis

3.2.1 Preparation of ligands and proteins

The GC-MS/MS results were obtained to find the most probable lead molecules present in HMPGL. The metabolites thus obtained, if were available in PubChem, then their structures were downloaded from the PubChem compound database (https://www.ncbi.nlm.nih.gov/pccompound) [21] in 3D conformation and .sdf format. The structures of few

Table 2. Bioactivity of 42 phytocompounds identified from the hydromethanolic extract of *Punica granatum* L. leaves by GC-MS/MS with more than 80% match score from the NIST Library.

S. No	Compound	Bioactivity and references
1	2-Furanmethanol or Furfuryl alcohol	Flavoring agent [27] and antioxidant [28]
2	2-Furancarboxaldehyde, 5-methyl-	Food additive and used for fragrance [29]
3	2,4-Dihydroxy-2,5-dimethyl-3(2H)-furan-3-one	Flavoring agent [30]
4	2H-Pyran-2,6(3H)-dione	Antiallergic [31], analgesic, mild sedative, soporific, fungicide, fungistatic, antihypoxic, spasmolytic, and muscle relaxant activities [32]
5	Benzyl alcohol	Antimicrobial activity [33]
6	2-Furancarboxylic acid	NR*
7	Maltol	Antitumor [34] and antinephrotoxicity activities [35]; alleviates hepatic fibrosis [36]
8	4H-Pyran-4-one, 5-hydroxy-2-methyl-	NR*
9	4H-Pyran-4-one, 2,3-dihydro-3,5-dihydroxy-6-methyl-	Alleviates male reproductive toxicity [37]; stimulates the autonomic nerve activity [38]; antiproliferative and pro-apoptotic [39]; antibiotic activities [40]
10	4H-Pyran-4-one, 3,5-dihydroxy-2-methyl- or 5-Hydroxymaltol	Nutrient [41]
11	Benzofuran, 2,3-dihydro-	Antiarrhythmic, spasmolytic, and antiviral activities [42]
12	5-Hydroxymethylfurfural	Antiinflammatory, antioxidant and antiproliferative activities [43]
13	1,2,3-Benzenetriol or Pyrogallol	Antitumor, cytotoxic and antiproliferative activities [44]
14	Syn-tricyclo(5.1.0.0(2,4))oct-5-ene, 3,3,5,6,8,8-hexamethyl-	NR*
15	Megastigmatrienone	Flavoring agent [45]
16	2-(3-Isopropyl-4-methyl-pent-3-en-1-ynyl)-2-methyl-cyclobutanone	NR*
17	n-Hexadecanoic acid or Palmitic acid	Antifungal [46] and antioxidant activities [47]
18	9,12-Octadecadienoic acid (Z,Z)- or Linoleic acid	Antimicrobial activity [47]
19	9,12,15-Octadecatrienoic acid, (Z,Z,Z)- or Alpha-linolenic acid	Regulates butyrylcholinesterase [48], antioxidant and antimicrobial [47]; antiinflammatory activities, antiacne, antiandrogenic, antiarthritic, antibacterial and anticandidal, anticancer, anticoronary, antieczemic, antihistaminic, hepatoprotective, hypocholesterolemic, insectifuge, nematicide, 5-alpha reductase inhibitor and cancer preventive activities [40]
20	Octadecanoic acid	Antimicrobial [40]
21	3-Furaldehyde	Inhibits polyphenol oxidase 2, phenolase, cresolase and tyrosinase [49]
22	1H-Inden-1-one, 2,3-dihydro-3,3,5,6-tetramethyl-	Antifungal activity [50]
23	1,1,4,5,6-Pentamethyl-2,3-dihydro-1H-indene	NR*
24	Benzoic acid, 4-ethoxy-, ethyl ester	Antimicrobial activity [40]
25	4,4,5,8-Tetramethylchroman-2-ol	Possible treatment against oligospermy and oliguria [45]
26	3-Hexadecyne	Antiandrogenic agent [51]
27	Hexadecanoic acid, methyl ester or Methyl palmitate	Prevents Kupffer cell activation [52]; antiinflammatory [53, 54] and antifibrotic activities [53]
28	9-Hexadecenoic acid	Regulates lipogenesis, desaturation, and β-oxidation in bovine adipocytes [55]
29	Phytol	Antioxidant [47], anticancer, antiinflammatory, antidiuretic, antimicrobial activities [40]; Fragrance [56] Antinociceptive activities [57]
30	Methyl stearate	Nutrient, membrane stabilizer and energy source [58]
31	Eicosanoic acid/Arachidic acid	Nutrient, membrane stabilizer and energy source [59]
32	Phthalic acid, octyl tridec-2-yn-1-yl ester	Antiplatelet activity [60]
33	Heptacosane	NR*
34	Squalene	Antitumor and anticancer effects [breast, colon, lung and ovarian cancer], hypocholesterolemic activity, reduces skin damage caused by UV radiation, cardioprotective effect and , detoxifying agent [61]
35	Alpha-Tocospiro A	NR*
36	Alpha-Tocospiro B	Cytotoxic [62] and α-Glucosidase inhibiting activities [63]
37	Sulfurous acid, hexyl pentadecyl ester	NR*
38	Carbonic acid, eicosyl vinyl ester	NR*
39	4-Hydroxy-2-methylacetophenone	Acaricidal activity [64]
40	2,5-Furandicarboxaldehyde	Insulin receptor partial antagonist [65]
41	4H-Pyran-4-one, 5-hydroxy-2-(hydroxymethyl)-methyl- or Kojic acid	Skin-lightening agent [inhibits tyrosinase] antioxidant, antidiabetic, anticancer, antiinflammatory, antimicrobial, antiproliferative, antiparasitic, antiviral, antitumor, antispeck, pesticidal,insecticidal, radio protective properties [66]
42	Hexadecanoic acid, 2-hydroxy-1- (hydroxymethyl)ethyl ester Or 2-Palmitoylglycerol	Food additive [67]

NR*, no activity reported.

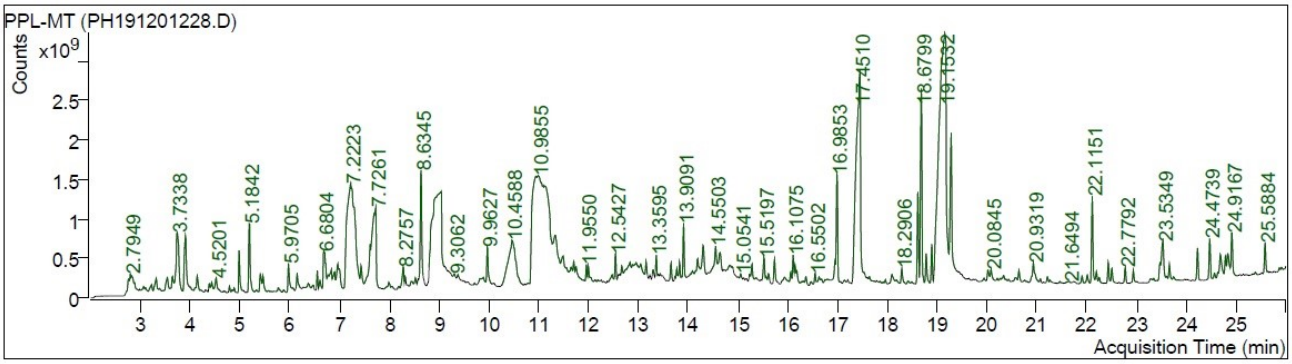

Fig. 1. GC-MS/MS chromatogram of the hydromethanolic extract of *Punica granatum* L. leaves.

metabolites, which were not available in PubChem, were obtained from NIST Library and sketched using ChemSketch. The standard protocols of BIOVIA Discovery Studio v3.5 (DS) software (Accelrys Software Inc., USA, 2012) was used for ligand preparation. This standard program was widely employed to prepare all the lead-like compounds to fix and resolve all different chemical properties such as different protonation states, ionization states, isomers, tautomers adding hydrogen, removing duplicates, and fixing bad valencies. This step is crucial because the receptor-ligand interactions have different protonation states; isomers and tautomers typically have different 3D geometries and binding characteristics.

This study is mainly centered on drug target proteins related to breast cancer; therefore, a list of principal biomarkers and prognostic biomarkers that were immunohistochemically tested in breast cancer tissue, are considered for the study [22]. A network of these proteins was constructed using a string database version 11.0 (https://string-db.org/) [23] and analyzed using Cytoscape, and the protein with a medium number of edges was used as a protein target. Basic sequence and structure analysis of the ER was conducted. The protein structures of the different isoforms of ER structure such as ERα LBD (PDB code 3ERD), ERβ LBD (PDB code 3OLS) and ERRγ LBD (PDB code 2GPU) were retrieved in .pdb formats from structural protein database (https://www.rcsb.org/) [24]. Initially, hetatoms and unbound water molecules were removed, following which, a CHARMM force field was applied. It removes alternative conformers and balances valencies of the amino acids. Subsequently, the protein predation protocol builds a loop and refines the side chain of proteins.

3.2.2 Absorption, Distribution, Metabolism, Excretion and Toxicity (ADMET) and drug-likeness screening

The 145 compounds identified through GC-MS/MS analysis were then subjected to a dual-step virtual screening process, in which, first, the compounds were screened for their pharmacokinetic activities, such as ADMET, which were predicted using ADMET Descriptors protocol in DS v3.5.

ADME studies are widely employed in drug discovery to optimize the properties to convert leads into drug molecules or medication. The lead compounds are mostly identified through virtual high-throughput screening approaches or by virtual screening. Drug discovery statistics reveal that around 50% of the drugs fail in the course of clinical trials due to nonstandard effectiveness (efficacy), which has low bioavailability due to poor intestinal absorption and undesirable metabolic stability [25]. The failure of drug-like candidates in the later stages of drug development proves very expensive. Therefore, to scale back the value and clinical failures of recent drug-like molecules, the lead compounds were screened within the initial stages for ADMET. Secondly, the ADMET screened compounds were checked for *Lipinski's rule of five (*RO5) violations to ensure that the compounds have drug-likeness properties [5]. Finally, the remaining compounds were taken for further process.

3.2.3 Protein-ligand docking

The docking study was performed by identifying the binding site of drug-target protein using the LibDock algorithm available in Discovery Studio 3.5. It uses protein binding site features to direct docking. It finds polar and apolar probes by placing a grid around the ligand 20 Å by 20 Å by 20 Å and extra space of 5 Å in each direction [26]. The site volume and binding site sphere will vary for all the three drug targets and were as follows; for ERα LBD 5.524X-0.284Y-5.750Z, ERβ LBD 25.17X-27.96Y-11.25Z and ERRγ LBD 62.44X-47.17Y-25.727Z. Bad hotspots were removed manually. Finally, pose optimization was done using Broyden-Fletcher-Goldfarb-Shanno (BFGS) and top-scoring ligand poses were ranked and retained.

3.2.4 Molecular dynamics and simulation (MDS)

The molecular dynamic simulation (MDS) was ideally carried out to inspect the stability and rationality of the binding patterns between the probable ligands and the specific target protein. The finest interaction hits obtained from receptor-ligand docking were used for MDS.

In this experiment, top pose and elite compound interaction with individual drug targets were simulated using the GROMACS version 2016 package [3, 7]. 3ERD-2-propenoic acid, 3-(4-hydroxyphenyl)-, methyl ester, 3OLS-2-propenoic acid, 3-(4-hydroxyphenyl)-, methyl ester and 2GPU-2-propenoic acid, 3-(4-hydroxyphenyl)-, methyl ester complex topologies were prepared separately for the protein and the ligand. For the ligand molecular topology, the coordinate files were generated by the PRODRG 2.5 server, followed by solvating the receptor-ligand complex in the dodecahedral box with a minimal distance of 1.0 nm. The whole protein-ligand complex and aqueous system are maintained at neutral conditions using Na^+ and Cl^-ions. Subsequently, the steepest descent algorithm was employed to implement a minimum of 1000 to a maximum of 50,000 steps of minimization to retain the proper distance between the atoms accompanied by no structural changes in the compound. The temperature of 300 K and pressure of 1 bar were attained by making use of canonical ensemble (NVT) and isothermal-isobaric ensemble (NPT) equilibration simulations of 500 ps. The time step of all stages was set to 2 fs. In the end, the protein-ligand complexes were subjected to 30 ns MDS. For further investigation of the stability and flexibility of the complexes, root mean square deviation (RMSD), root mean square fluctuation (RMSF), the radius of gyration (Rg), and hydrogen bonds were analyzed through graphical representation.

4. Results

4.1 *In-vitro* analyses

4.1.1 Extract yield, preliminary phytochemical analysis and antioxidant activity

The % yield of the HMPGL was found to be 1.44%. Qualitative phytochemical analysis revealed the absence of resins and the presence of alkaloids, carbohydrates, coumarins, flavonoids, glycosides, saponins, steroids, tannins, fatty acids, phenols and terpenoids. The IC_{50} value for the antioxidant activity of the extract based on the DPPH free radical scavenging assay was identified to be 3.12 mg/L and was comparable with the standard quercetin (3.91 mg/L). Phenol content of the HMPGL found to be 86.17 $\pm$ 3.67 mg gallic acid equivalent 100 g^{-1} dry weight.

4.1.2 GC-MS/MS profiling

Fig. 1 indicates the GC-MS/MS chromatogram of the HMPGL. After comparing mass spectra of the components with the NIST Library, 145 phytocompounds were identified and listed in Table 1. Out of the 145 compounds screened, 102 and 42 compounds (Table 2, Ref. [27–67]) were identified to have more than 80% match with NIST library, respectively. Among the screened compounds, 19 were identified as novel metabolites. The most prevailing compounds among the 145 metabolites are 9,12,15-octadecatrienoic acid, (Z,Z,Z)- (linolenic acid), 1,2,3-benzenetriol(pyrogallol), n-hexadecanoic acid (palmitic acid), maltol, 5-hydroxymethylfurfural, 4H-Pyran-4-one, 2,3-dihydro-3,5-dihydroxy-6-methyl-, undecanol-5 and 3-furaldehyde. These phytocompounds are different fatty acids, terpenes, heterocyclic compounds, flavonoids, pyrrolidines, sesquiterpenoids and phenols. The mass spectrum corresponding to the structure of 2-propenoic acid, 3-(4 hydroxyphenyl)-, methyl ester (also known as 4-coumaric acid methyl ester), which exhibits the highest binding affinity with the breast cancer receptors considered in the current investigation, was represented in Fig. 2.

4.2 Computational analysis

4.2.1 Sequence and structure assessment of estrogen receptors and their related ligand-binding domains

The protein network of text mined and experimental interactions; and interaction score with 0.9 confidence, consisted of 81 number of nodes and 234 edges with a *P*-value of $<1.0^{e-16}$, 0.072, network density and 0.919 network heterogenicity. The network revealed Tumor protein 53 (TP53), RAC-alpha serine/threonine-protein kinase (AKT1), cyclin D1(CCND1), epidermal growth factor receptor (EGFR), phosphatase and tensin homolog deleted on chromosome 10 (PTEN), human epidermal growth factor receptor 2 (ErbB2/HER2), DNA mismatch repair protein (MSH2) and MYC as the hub proteins and ER as a suitable drug target with a medium number of edges, a middle degree node, 0.533 closeness centrality and 0.13 clustering coefficient (Fig. 3).

With the advent of new technology and computational tools, there is a massive increase in the deposition of protein structures in PDB. This consequently creates an increased level of difficulty in selecting an optimal PDB entry for docking. X-ray crystallographic structures of ERα LBD (PDB ID:3ERD), ERβ LBD (PDB ID:3OLS) and ERRγ LBD (PDB ID: 2GPU) were selected after a thorough screening of 329 entries of ER' structures with a minimum resolution, no missing atoms and completeness of the binding domain. The ERα LBD, ERβ LBD and ERRγ LBD have orthogonal bundle architecture. They mainly consist of α-helix, belong to the family of nuclear receptor and exhibited retinoid-X-receptor topology. Largely, there are numerous conserved regions observed in-between the three sequences. However, ERα LBD and ERβ LBD showed 83.5% sequence and structure similarities, whereas ERRγ-ERα and ERRγ-ERβ showed a similarity of 62.2% and 61.5%, respectively. Overall, multiple sequence alignment showed 55.7% similarity between the three LBDs of ERα, ERβ and ERRγ. The raw protein structures were refined using a protein preparation tool prior to molecular docking. A loop of ERβ and ERα was built based on SEQRES data, the atoms were arranged, and its side chains were refined using PDB data. Notably, the structural analysis also revealed that the binding pocket of ERα is larger and broader than that of ERβ (Fig. 4).

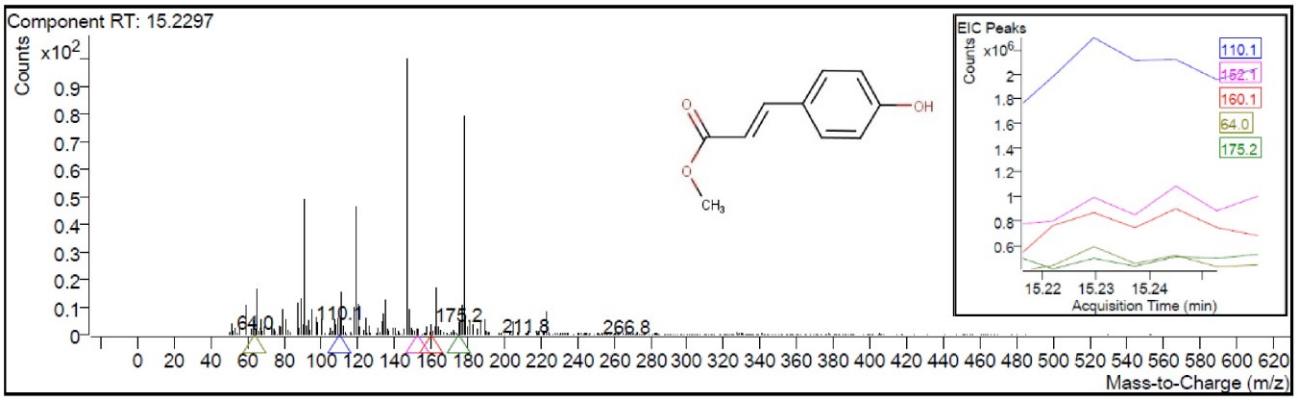

Fig. 2. Mass spectrum of the component (2-propenoic acid, 3-(4-hydroxyphenyl)-, methyl ester) at retention time (RT) 15.2297 (represented in the insert) with a *y*-axis scale from 0 to 0.9 $\times$ 10^2 and its structure identified in hydromethanolic extract of *Punica granatum* L. leaves by GC-MS/MS. Extracted ion chromatogram (EIC) peaks is the same component spectrum at a scale from 0.6 to 2.0 $\times 10^6$ (insert). Molecular formula: $C_{10}H_{10}O_3$, Molecular weight: 178.18.

4.2.2 *In-silico* pharmacokinetics properties and Lipinski's rule (RO5) validation

Efficacy and toxicity are the pivotal determinants of successful drug development. Therefore, all the GC-MS/MS characterized metabolites were subjected to the virtual screening process thoroughly. Initial screening with Absorption, Distribution, Metabolism, Excretion and Toxicity (ADMET) drastically narrowed down the count of molecules (Figs. 5,6) followed by RO5 violation AlogP $\leq$5, with molecular weight $\leq$500, hydrogen bond donor $\leq$5, and hydrogen bond acceptor $\leq$10 were evaluated to justify their drug-likeness behaviour. Fig. 5 represents the pharmacokinetic profile of all the metabolites identified in HMPGL. Out of 145 compounds analyzed, 77 revealed good and optimal solubility with a score of 3 and 4. Total, 103 molecules demonstrated high, medium and low blood-brain barrier (BBB) penetration. The human intestinal absorption of 109 compounds was 0 and 1, indicating good and moderate absorption of these hits (Fig. 5). 125 compounds were non-inhibitors of CYPD26, 96 were nontoxic to liver cells and 50 exhibited low binding affinity to plasma proteins. The 16 and 47 compounds showed no carcinogenicity in female and male rats, respectively. 122 compounds were non-mutagens in TOPKAT screening (Fig. 6). Therefore, systematic analysis of all these pharmacokinetic properties revealed only nine compounds that are nontoxic and safe. Among them, 9,12,15-octadecatrienoic acid, 2,3-dihydroxypropyl, ester (Z,Z,Z)- and hexadecanoic acid, 2-hydroxy-1-(hydroxymethyl)ethyl ester were not drug-like molecules as their AlogP were 'greater than five' (violation of *Lipinski's* RO5). However, 19 novel metabolites were not docked against the ER due to their limitation of exhibited carcinogenicity based on *in-silico* prediction.

Detailed tabulations of the screened compounds, which completely satisfied the ADMET properties and drug-likeness, are given in Table 3. It is evident from the table that the standard drug, tamoxifen, an anti-estrogen that is widely used in the clinic to treat ER-positive breast tumors) violated both RO5 and exhibits hepatotoxicity and high affinity to plasma binding proteins. 2-Propenoic acid, 3-(4-hydroxyphenyl)-, methyl ester, a natural compound, followed RO5 and did not exhibit any toxicity in ADMET prediction suggesting its efficacy and nontoxic nature. Some of the natural compounds of HMPGL also showed hepatotoxicity and affinity to plasma proteins.

4.2.3 Binding and interaction analysis

The screened compounds and the standard drug tamoxifen were docked with three different ER structures. The docked poses were examined based on the LibDock score (Kcal/mol) and various types of interactions in hydrogen/hydrophobic interaction analyses. The structural conformations of 4-coumaric acid methyl ester (92203) were the most favorable for the binding cavity of all the three receptors, especially hydroxyl group (-OH) exhibits a major structure-activity relationship, where the removal of (-OH) in the para position of the structure is directly proportional to dock score values. Thus, this position is considered crucial for the binding of this phytochemical to these receptors. Other compounds like benzoic acid, 3,4,5-trihydroxy-, methyl ester (7428), 2-propanone,1-hydroxy-3-(4-hydroxy-3-methoxyphenyl) (586459), (4H)4a,5,6,7,8,8a-hexahydrobenzopyran-5-one-3-carboxamide,2-(2-hydroxypentyl)-8a-methoxy-4a-methyl (587806) and tamoxifen (2733526) also showed favorable binding, but the standard drug tamoxifen violated the RO5 and demonstrated toxicity. The structure of 4-coumaric acid methyl ester showed high complementarity to αLBD with a docking score of 75.16 kcal/mol, whereas γLBD is favorable for tamoxifen. Nevertheless, βLBD was structurally compatible with both 4-coumaric acid methyl ester and tamoxifen, as represented in Fig. 7.

Fig. 3. Protein interaction network of principal and prognostic biomarkers of breast cancer.

The binding pattern and chemical interactions of nontoxic natural 4-coumaric acid methyl ester present in HMPGL with good docking score, with the three isoforms of ER, were demonstrated in Fig. 8. The α (W393, E353, R394, L449 and E323) and β (F356, L343, L339 and A302) LBD residues are considered as crucial active site amino acids for ligand binding and responsible for antagonist activity. R394 of α binding domain makes crucial Pi interactions with the ligand. In contrast, R316 and L309 amino acids play a vital role in ERRγ LBD. In αLBD, 4-coumaric acid methyl ester interacts with W393, R353, R394, L449 and E323 to form strong hydrogen interaction and Pi-cation, respectively, whereas, with β and related γ, it forms hydrogen bonding with F356 and R316, and L309, respectively. In all these interactions, -OH forms hydrogen bond interaction; so, it can be considered as an active pharmacophore for 4-coumaric acid methyl ester.

4.2.4 Time-dependent parameter analysis

A time-dependent MD simulation at 50 ns was conducted using GROMACS 2016 to investigate the flexibility and overall stability of docked complexes. MD simulation were carried for the best candidate molecule, 4-coumaric acid methyl ester, with three drug target receptors and time-dependent parameters, were analyzed as described by Dhivya *et al*., 2018 [3]. The root mean square deviation (RMSD), the radius of gyration (Rg) and hydrogen bond (H-bond) interaction graphs were generated by using Xmgrace software in a Linux environment (Fig. 9).

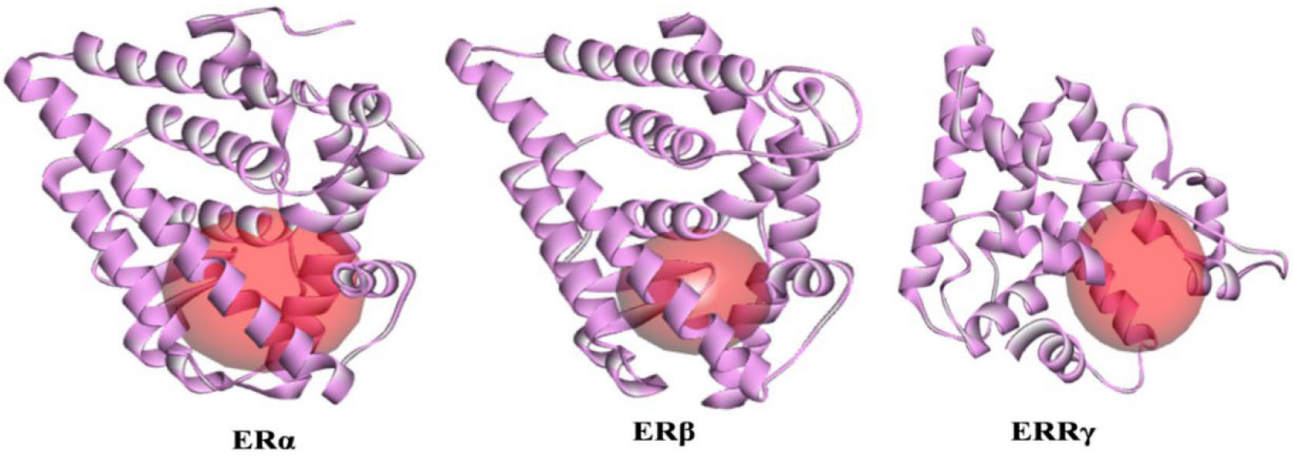

Fig. 4. Active site representation of isomers of human estrogen receptor.

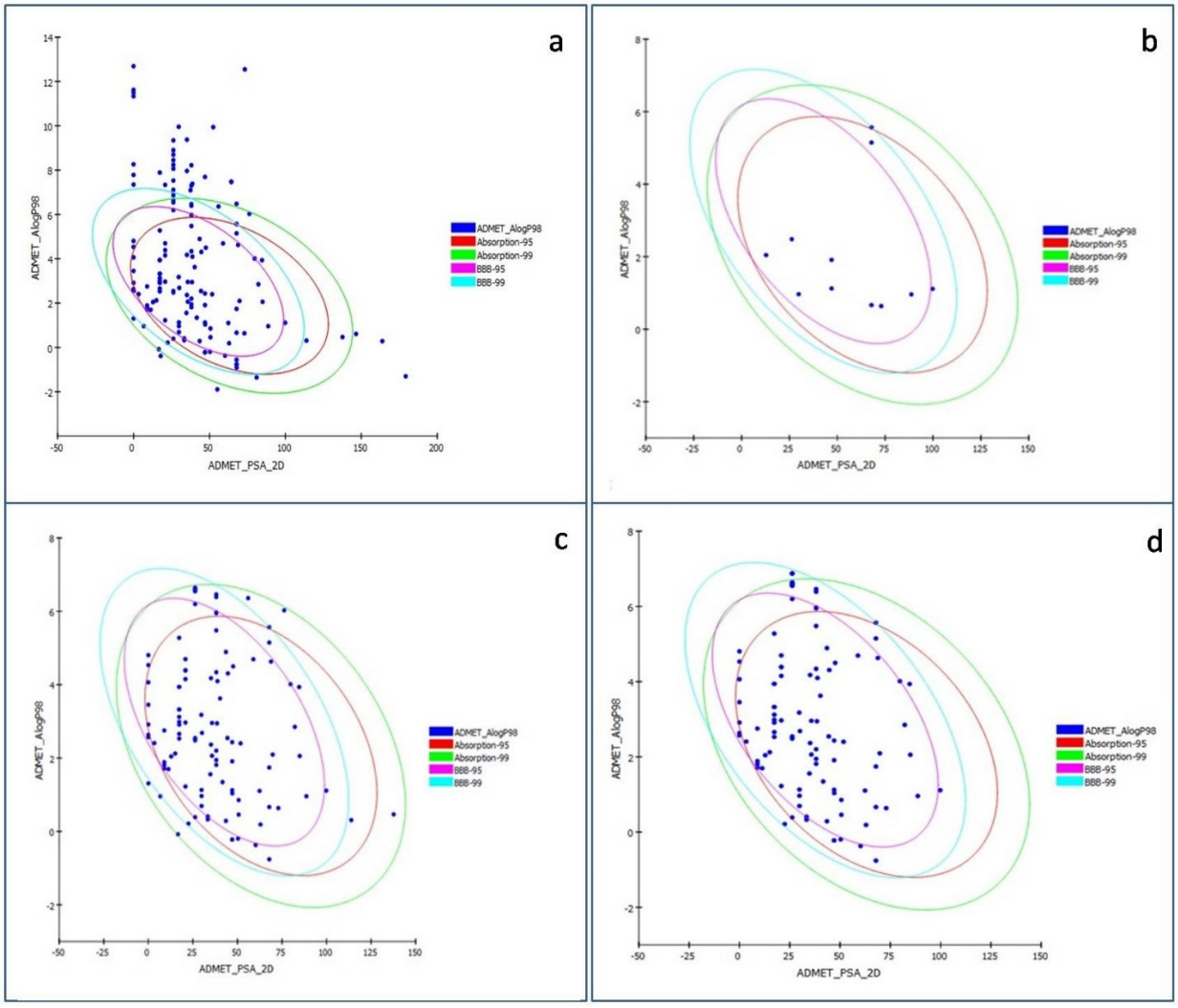

Fig. 5. The graph of ADMET 2D polar surface area (PSA_2D) vs. ALogP of 145 phytochemicals of *Punica granatum* L. representing the confidence limit ellipses of 95% and 99% corresponding to the intestinal absorption models and blood-brain barrier (BBB). (a,b) represent molecules before and after ADMET screening. (c) The ellipses define regions where well-absorbed Human Intestinal Absorption (HIA) compounds are expected to be found after oral administration. (d) The graph represents compounds with low and medium blood-brain barrier (BBB) penetration.

Table 3. Predicted drug-likeness and ADMET properties of phytoconstituents from hydromethanolic extract of *Punica granatum* L. leaves.

Compounds ID	RO5	Solubility level	BBB level	Absorption	CYPD26	Hepatotoxic	PPB	NTP Female & male rat	Ames mutagen
7428	Y	4	3	0	F	F	F	NC	NM
14334	Y	3	3	0	F	F	F	NC	NM
85447	Y	4	1	0	F	F	F	NC	NM
92203	Y	4	2	0	F	F	F	NC	NM
586459	Y	4	3	0	F	F	F	NC	NM
587806	Y	3	3	0	F	F	F	NC	NM
6432173	Y	3	1	0	F	F	F	NC	NM
2733526									
Tamoxifen (Standard drug)	N	1	0	1	T	T	T	NC	NM

RO5 (*Lipinski's rule of five*): Y, Yes (Follow RO5); N, No (Don't follow RO5). Solubility level: (1) No; (2) Very low but possible; (3) Good; (4) Optimal. BBB (Blood Brain barrier): (0) Very high penetrant; (1) High Medium; (2) Medium; (3) Low. Human Intestinal Absorption: (0) Good; (1) Moderate. CYP2D6: F, False (Non-binding); T, True (Binding). Hepatoxicity: T, True (Toxic); F, False (Nontoxic). PPB (Plasma protein binding): F, False (Non-binding); NC, Non-carcinogen; NM, Non-mutagen.

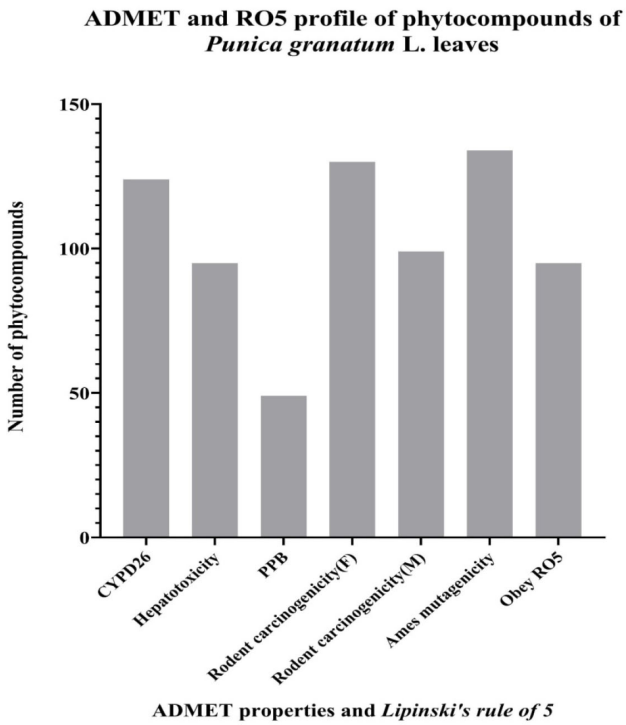

Fig. 6. Number of phytocompounds of hydromethanolic extract of *Punica granatum* L. leaves predicted to be CYPD26 inhibitors, non hepatotoxic, no plasma protein binding (PPB) affinity, non-carcinogens in Female (F) and Male (M) non-mutagens and obey RO5.

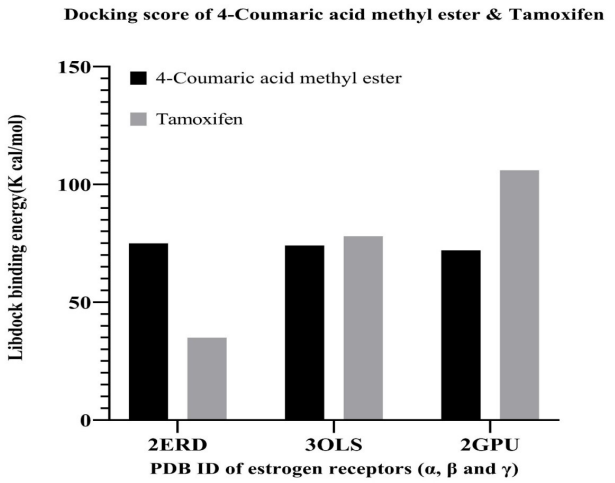

Fig. 7. The binding energy of 4-coumaric acid methyl ester present in hydromethanolic extract of *Punica granatum* L. leaves and tamoxifen with three isoforms of estrogen receptor (3ERD, 3OLS and 2GPU corresponds to the PDB ID of the LBDs of ERα, ERβ and ERRγ, respectively).

As is evident in Fig. 9a.1, the increasing trend of RMSD was observed for all the six complexes, 3ERD/ERα LBD–4-coumaricacid methyl ester, 3OLS/ERβ LBD–4-coumaricacid methyl ester, and 2GPU/ERRγ LBD–4-coumaricacid methyl ester, having diverse RMSD values 0–0.30. Initially, the ERα LBD complex showed little jiggling, whereas ERβ LBD showed high fluctuations, but ERRγ LBD exhibited a gradual increase in RMSD until 10 ns. The fluctuations of the ERα LBD complex were between 0.10 to 0.30 nm, but after 30 ns, this complex attained stability with slight deviations in RMSD value. However, the fluctuations of the ERβ LBD complex elevated up to 0.25 nm at 5 ns, dropped to 0.2 nm at 12.5 and 20 ns, with a sudden drop of RMSD to 0.2 nm at around 12.5 and 20 ns, fluctuated till 35 ns and steadily increased at the end of dynamics. The RMSD of the ERRγ LBD complex gradually increased until 35 ns and attained plateau, which was in the range of 0–0.2. The Rg analysis usually measures the compactness of a protein or system. The predicted results in Fig. 9b.1 demonstrated that all the three complexes ERα LBD, ERβ LBD and ERRγ LBD- were static and

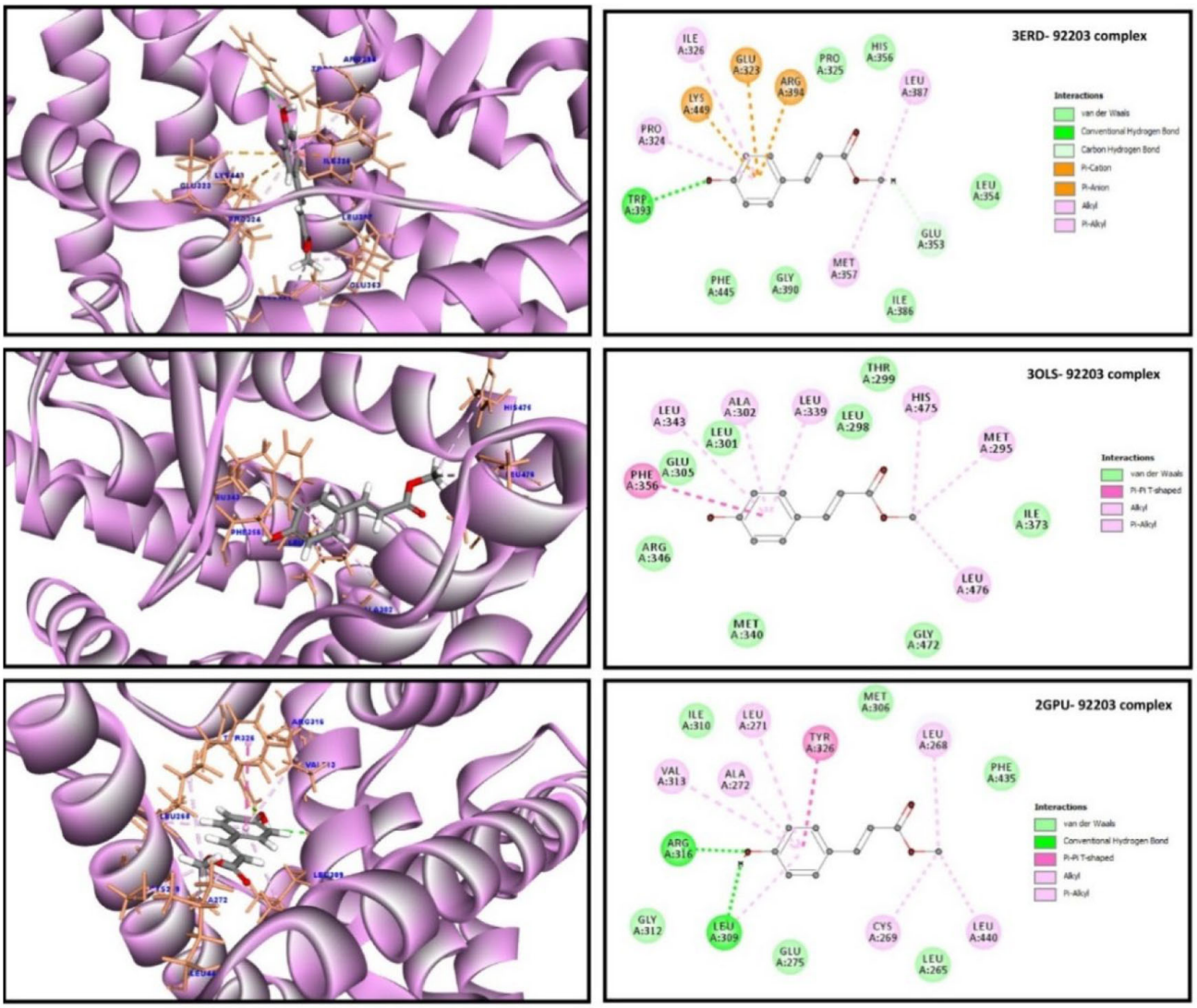

Fig. 8. Both 3D and 2D docked representation 4-Coumaric acid methyl ester with three different estrogen receptors' (drug targets) active sites. 4-Coumaric acid methyl ester docked with 3ERD (the ligand-binding domain of ERα; A&B), 3OLS (the ligand-binding domain of ERβ; C&D), and 2GPU (the ligand-binding domain of ERRγ; E&F).

constant with Rg values 1.8 to 1.85 nm, 1.775 to 1.825 and 1.750 to 1.850 nm, respectively, throughout the simulation time 0–50 ns, the complexes slightly fluctuated to attain its stability. Comparative MD simulations revealed that the residual backbone and appropriate conformation of the ERα LBD complex was stable compared to other complexes. The H-bond plot of the simulation was presented in Fig. 9c.1. It is practically impossible to inspect H-bond stability by examining the crystal, nuclear magnetic resonance (NMR), and electron microscopy-solved structures. Consequently, it is significant to probe the stability of the H-bonds utilizing MD simulations. The presence of H-bond interactions in the docked complexes was identified by the gmx hbond tool in the accepted geometry (distance $<$3.5 Å and 180° $\pm$ 30°, between the donor and acceptor). H-bonds between the ligand and the receptor jiggled all through the simulation. The maximum number of H-bonds bound confirmation for ERα LBD, ERβ LBD and ERRγ LBD complexes are 3, 3 and 4, respectively. It is evident from the 3ERD/ERα LBD–Tamoxifen, 3OLS/ERβ LBD–Tamoxifen, and 2GPU/ERRγ LBD–Tamoxifen, having diverse RMSD values 0–0.30. (Fig. 9a.2). All the three complexes exhibited higher stability compared to complexes represented in Fig. 9a.1. From Fig. 9b.2 it can be noted that 3OLS/ERβ LBD–Tamoxifen was more stable all through the run. Only 3OLS/ERβ LBD–Tamoxifen showed H interactions.

5. Discussion

Breast cancer is regarded as one of the major burdens observed in women. Consequently, there is an upsurge in efforts for the discovery of new drugs to combat this disease. Plants are widely regarded as a reservoir of various

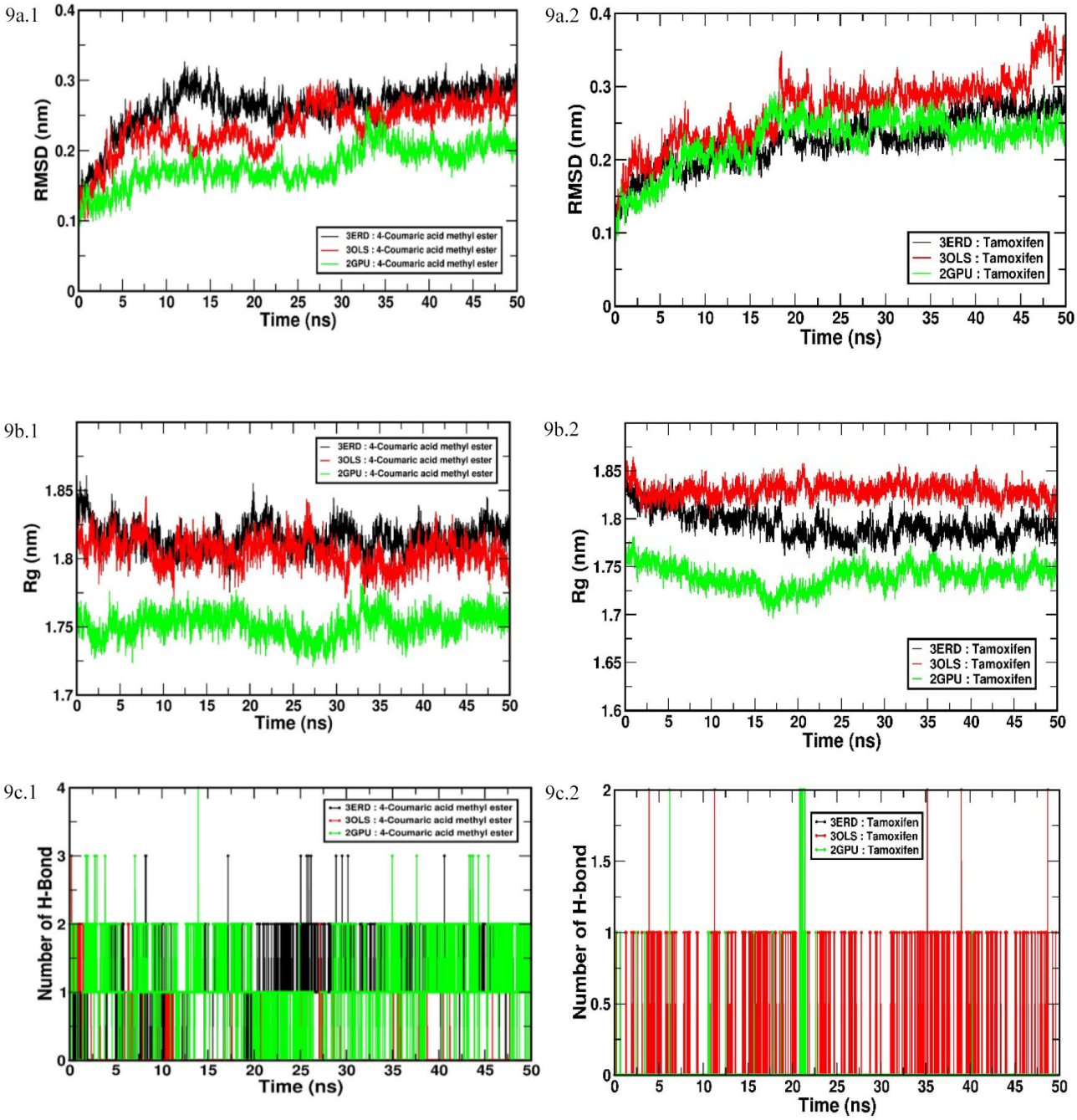

Fig. 9. Time-dependent MD and simulation of 4-coumaric acid methyl ester and tamoxifen with three different ERs' (drug targets) active sites (LBD of ERα, ERβ and ERRγ). (a) Root mean square deviation (RMSD) plot. (b) Radius of gyration (Rg) plot. (c) Hydrogen bond (H-bond) plot.

types of bioactive metabolites with various therapeutic and pharmacological potentials [68]. Due to their diverse nature, several plant-based molecules are used as drugs and are in the process of discovery routes [69]. Most of the research studies reported to date involved the characterization of peel, seed and bark by GC-MS and very few studies on leaves of *Punica granatum* L. using the NMR technique. However, no studies have been reported on leaves by GCMS analysis. Notably, in the present study, we attempted to characterize the possible phytochemicals exclusively by GCMS in *Punica granatum* L. leaves [70, 71]. The present study identified 145 phytoconstituents from HMPGL by GC-MS profiling. Similar to our report, 5-hydroxymethylfurfural was reported in high concentrations in ethyl acetate extract of the fruit peel of *Punica granatum* by Barathikannan *et al*. (2016) [71]. These phytochemicals are known to contribute to the diverse medicinal properties of the plant, as previously reported [69]. A majority of these phytocompounds were reported to have antioxidant, antiinflammatory, anticancer, and antimicro-

bial activities, and used as food additives (Table 1). Due to the presence of alkaloids, coumarins, flavonoids, glycosides, phenols, saponins, tannins and terpenoids, HMPGL has better DPPH radical scavenging activity. Bekir *et al*. (2013) [72] had previously reported the antioxidant potential of *Punica granatum* L. leaves extracted with different solvents based on their polarity.

Using the *in-silico* approach, the pharmacokinetics and toxicity studies of compounds are investigated before evaluating their biological activity [73, 74]. Poor pharmacokinetic profile and toxicity are the main reasons for last stage failures in drug discovery. Therefore, in the present study, all the identified 145 phytochemicals from the HMPGL were initially screened for ADMET and *Lipinski's* RO5, and only eight molecules were identified to be drug-like nontoxic molecules. Among the 138 phytoconstituents, a majority of them were identified to be fatty acids and terpenes. Due to the presence of the long hydrophobic -acyl chains and terpenes, the fatty acids exhibited low solubility and high affinity to plasma binding proteins indicating low efficacy. They will be highly toxic as they can penetrate BBB, bind to CYPD26 and exhibit hepatotoxicity.

Docking studies were carried out with 51 metabolites (eight drug-like nontoxic molecules + 42 mentioned in Table 1). Those 42 metabolites were also used for docking studies as most of them exhibited hepatotoxicity, and it is one very common toxic property noted in many FDA-approved drugs like tamoxifen. One of the most important steps in developing a new lead molecule is target selection. Systematic analysis of protein interaction networks (disease networks) and identification of hub protein enhances the understanding of the molecular basis of the disease. They also help in determining the key node as a potential target protein in the drug discovery process. Several hub proteins have been identified to be not suitable as drug targets as their inhibition may affect crucial activities of the cell; However, ER, a middle degree node and with high cluster coefficient, is an optimal drug target for breast cancer treatment [75, 76]. Our binding pocket analysis revealed that ERα is larger and broader than ERβ, which has been previously speculated to be due to the possible sequence diversity of ER Paterni *et al*. (2014) [77]. Targeting more than one receptor helps in an in-depth understanding of the efficacy and toxicity of the drugs, including complex interactions [78]. So, in this study, we exclusively focused on three significant receptors involved in breast cancer mechanisms (ERα, ERβ and ERRγ). In our docking results, there was notable variation seen in the binding energies with the three receptors for all the docked molecules and these differences can be attributed to selective binding of the phytoconstituents to the diverse LBDs of these receptors. In all the interactions, the amino acids Arg, Leu and Glu of the LBD were making crucial interactions with the ligand (4-coumaric acid methyl ester). Interestingly Arg394 alpha binding domain has been reported to make crucial pi interactions with the ligand [79]. The deletion of the -OH of the 4-coumaric acid methyl ester reduces the binding affinity. Hence, it can be considered a pharmacophoric feature due to its hydrogen bonding with the receptors.

MD simulations of the docked complexes from docking studies help refine docking and enhance the accuracy of the binding affinity predictions [3, 68]. Post docking MD simulations at 50ns reflected the time-dependent behaviour of the docked complexes. The ligand in the ERRγ LBD complex was having the least RMSD values and attained stability at 30 ns and remained stable till the end compared to ERβ LBD and ERα LBD complexes. The Rg values are almost in the same range (1.75 to 1.85) for all the complexes, whereas the ERRγ LBD complex with minimal vibrations, fluctuations, maximum H-bonds depicts its greater stability compactness and binding affinity with 4-coumaric acid methylester. This compound is a natural phenylpropenoic acid compound, belonging to a class of phenolic acids and is a phenolic antioxidant. The antioxidant potential of this compound might contribute to the anticancer effect against breast cancer plausibly due to its high binding affinity to ERα, ERβ and ERRγ LBDs.

6. Conclusions

To conclude, the current research work was an attempt to draw insight into the structural, functional, and dynamical aspects of phytocompounds of *Punica granatum* L. In the process, the GC-MS/MS metabolite profiling revealed the presence of 145 compounds. These can be deployed to discover novel drugs against various cancers, as *Punica granatum* L. is reported to have anticancer properties. Estrogen receptor plays a crucial role in cellular proliferation and differentiation of breast cancer cells, which was identified as a novel target for breast cancer by network pharmacology. 96% of the phytoconstituents exhibited toxicity in the virtual ADMET screen, and 35% did not exhibit drug-likeness. *In-silico*, molecular docking was performed against three isoforms of ER and compared with the standard drug tamoxifen. 4-Coumaric acid methyl ester, a nontoxic natural, demonstrated the highest affinity with core residues of 3ERD (ERα LBD), with 3OLS (ERβ LBD), with 2GPU (ERRγ LBD). Thus, the docking poses of the identified hit, 4-coumaric acid methyl ester, were further evaluated by dynamic simulation at 50 ns. Among the various ER receptors, the 2GPU complex, which is ERRγ LBD, is "the best" with minimum RMSD, constant Rg and maximum number of H-bonds indicating a stable and compact system. The presence of 4-coumaric acid methyl ester and various other bioactive metabolites reported justifies the use of *Punica granatum* L. for treating breast cancer by traditional practitioners. Taken together, our results represent a promising starting point for the preclinical evaluation of 4-coumaric acid methyl ester as a possible treatment for breast cancer.

7. Author contributions

SKM and KRS conceived the idea. TU performed *in-vitro* and computational studies and drafted the manuscript. DS assisted in *in-silico* experimentations. AKG helped in the experimental procedure and partially drafted the manuscript. HSY helped in the computational facility and wrote a part of the manuscript. DB helped in GC-MS/MS analysis and thoroughly revised the manuscript. SKM arranged the funds and supervised the whole study, edited, and upgraded the final version of the manuscript. All the authors analyzed, discussed the results, and approved the version to be submitted.

8. Ethics approval and consent to participate

Not applicable.

9. Acknowledgment

The authors acknowledge Neoscience Labs Private Limited, Chennai, India for allowing to utilize their GC-MS facility and their technical support. DBT-BIF computational facility and BiSEP facility at MLACW was used to carry out the research work. Dhivya also expresses her sincere thanks for the fellowship provided by the DBT-BIF facility at MLACW by Govt of India. The authors are grateful to Dr. V.R. Devraj, Professor, Bangalore Central University and Dr. C.S. Karigar, Professor, Bangalore University, India, for their valuable suggestions. This publication was supported by the Deanship of Scientific Research at Prince Sattam Bin Abdulaziz University, Al-kharj, Saudi Arabia.

10. Funding

This research was partially supported by a minor research grant (MLACW-MRP-057) from MLACW, Bengaluru, India.

11. Conflict of interest

The authors declare no conflict of interest.

12. Sample availability

The pomegranate extract samples are available with the authors.

13. References

[1] Usha T, Middha SK, Kukanur AA, Shravani RV, Anupama MN, Harshitha N, *et al*. Drug repurposing approaches: Existing leads for novel threats and drug targets. Current Protein & Peptide Sciences. 2020. (in press)

[2] Sliwoski G, Kothiwale S, Meiler J, Lowe EW. Computational methods in drug discovery. Pharmacological Reviews. 2014; 66: 334–395.

[3] Dhivya S, Suresh Kumar C, Bommuraj V, Janarthanam R, Chandran M, Usha T, *et al*. A study of comparative modelling, simulation and molecular dynamics of CXCR3 receptor with lipid bilayer. Journal of Biomolecular Structure & Dynamics. 2018; 36: 2361–2372.

[4] Middha S, Usha T, Pradhan S, Goyal A, Dhivya S, Prashanth Kumar H, *et al*. Molecular simulation-based combinatorial modeling and antioxidant activities of zingiberaceae family rhizomes. Pharmacognosy Magazine. 2017; 13: S715–S722.

[5] Usha T, Shanmugarajan D, Goyal AK, Kumar CS, Middha SK. Recent updates on computer-aided drug discovery: time for a paradigm shift. Current Topics in Medicinal Chemistry. 2017; 17: 3296–3307.

[6] Thomford NE, Senthebane DA, Rowe A, Munro D, Seele P, Maroyi A, *et al*. Natural products for drug discovery in the 21st century: innovations for novel drug discovery. International Journal of Molecular Sciences. 2018; 19: 1578.

[7] Middha SK, Usha T, Pande V. A Review on Antihyperglycemic and antihepatoprotective activity of eco-friendly punica granatum peel waste. Evidence-Based Complementary and Alternative Medicine. 2013; 2013: 656172.

[8] Lei F, Zhang XN, Wang W, Xing DM, Xie WD, Su H, *et al*. Evidence of anti-obesity effects of the pomegranate leaf extract in high-fat diet induced obese mice. International Journal of Obesity. 2007; 31: 1023–1029.

[9] Li Y, Yang F, Zheng W, Hu M, Wang J, Ma S, *et al*. *Punica granatum* (pomegranate) leaves extract induces apoptosis through mitochondrial intrinsic pathway and inhibits migration and invasion in non-small cell lung cancer *in vitro*. Biomedicine & Pharmacotherapy. 2016; 80: 227–235.

[10] Deng Y, Li Y, Zheng T, Hu M, Ye T, Xie Y, *et al*. The extract from *Punica granatum* (Pomegranate) Leaves promotes apoptosis and impairs metastasis in prostate cancer cells. Sichuan Da Xue Xue Bao Yi Xue Ban. 2019; 49: 8–12. (In Chinese)

[11] Marques LCF, Pinheiro AJMCR, Araújo JGG, de Oliveira RAG, Silva SN, Abreu IC, *et al*. Anti-inflammatory effects of a pomegranate leaf extract in LPS-induced peritonitis. Planta Medica. 2016; 82: 1463–1467.

[12] Amri Z, Ghorbel A, Turki M, Akrout FM, Ayadi F, Elfeki A, *et al*. Effect of pomegranate extracts on brain antioxidant markers and cholinesterase activity in high fat-high fructose diet induced obesity in rat model. BMC Complementary and Alternative Medicine. 2017; 17: 339.

[13] Trabelsi A, El Kaibi MA, Abbassi A, Horchani A, Chekir-Ghedira L, Ghedira K. Phytochemical study and antibacterial and antibiotic modulation activity of *Punica granatum* (pomegranate) leaves. Scientifica. 2020; 2020: 8271203.

[14] de Oliveira JFF, Garreto DV, da Silva MCP, Fortes TS, de Oliveira RB, Nascimento FRF, *et al*. Therapeutic potential of biodegradable microparticles containing *Punica granatum* L. (pomegranate) in murine model of asthma. Inflammation Research. 2013; 62: 971–980.

[15] Usha T, Goyal AK, Lubna S, Prashanth H, Mohan TM, Pande V, *et al*. Identification of anti-cancer targets of eco-friendly waste *Punica granatum* peel by dual reverse virtual screening and binding analysis. Asian Pacific Journal of Cancer Prevention. 2014; 15: 10345–10350.

[16] World Health Organization. Preventing cancer. 2021. Available at: https://www.who.int/cancer/detection/breastcancer/en/ (Accessed: 20 June 2020).

[17] Brueggemeier RW, Richards JA, Petrel TA. Aromatase and cyclooxygenases: enzymes in breast cancer. The Journal of Steroid Biochemistry and Molecular Biology. 2003; 86: 501–507.

[18] Adams LS, Zhang Y, Seeram NP, Heber D, Chen S. Pomegranate ellagitannin-derived compounds exhibit antiproliferative and antiaromatase activity in breast cancer cells *in vitro*. Cancer Prevention Research. 2010; 3: 108–113.

[19] Goyal AK, Middha SK, Sen A. Evaluation of the DPPH radical scavenging activity, total phenols and antioxidant activities in

Indian wild Bambusa vulgaris. Journal of Natural Pharmaceuticals. 2010; 1: 40.
[20] Velavan S: Phytochemical techniques—a review. World Journal of Scientific Research. 2015; 1: 80–91.
[21] National Center for Biotechnology Information. 2020. Available at: https://www.ncbi.nlm.nih.gov/pccompound (Accessed: 20 June 2020).
[22] Bertozzi S, Londero AP, Seriau L, Vora RD, Cedolini C, Mariuzzi L. Biomarkers in breast cancer, in biomarker-indicator of abnormal physiological process. IntechOpen. 2018; 1–28.
[23] String. 2020. Available at: https://string-db.org/ (Accessed: 20 June 2020).
[24] RCSB Protein Data Bank. A Structural View of Biology. 2020. Available at: https://www.rcsb.org/ (Accessed: 20 June 2020).
[25] Li AP. Screening for human ADME/Tox drug properties in drug discovery. Drug Discovery Today. 2019; 6: 357–366.
[26] Diller DJ, Merz KM. High throughput docking for library design and library prioritization. Proteins: Structure, Function, and Genetics. 2001; 43: 113–124.
[27] Okaru AO, Lachenmeier DW. The food and beverage occurrence of furfuryl alcohol and myrcene-two emerging potential human carcinogens? Toxics. 2017; 5: 9.
[28] Kim MK, Nam P, Lee S, Lee K. Antioxidant activities of volatile and non-volatile fractions of selected traditionally brewed Korean rice wines. Journal of the Institute of Brewing. 2014; 120: 537–542.
[29] The Metabolomics Innovation Centre. Showing metabocard for 5-Methyl-2-furancarboxaldehyde (HMDB0033002). 2019. Available at: https://hmdb.ca/metabolites/HMDB0033002 (Accessed: 20 June 2020).
[30] Chukwu CJ, Omaka ON, Aja PM: Characterization of 2,5-dimethyl-2,4-dihydroxy-3(2H) furanone, a flavourant principle from sysepalum dulcificum. Natural Products Chemistry and Research. 2017; 5: 1000299.
[31] Garst ME, Gluchowski C, Kaplan LJ: U.S. Patent No. 4,725,620. Washington, DC, U.S. Patent and Trademark Office. 1988.
[32] Novikov DV, Yakovlev IP, Zakhs VE, Prep'yalov AV. Synthesis, properties, and biological activity of 4-Hydroxy-2H-pyran-2-ones and their Derivatives. Russian Journal of General Chemistry. 2002; 72: 1601–1615.
[33] Yano T, Miyahara Y, Morii N, Okano T, Kubota H. Pentanol and benzyl alcohol attack bacterial surface structures differently. Applied and Environmental Microbiology. 2015; 82: 402–408.
[34] Li W, Su X, Han Y, Xu Q, Zhang J, Wang Z, *et al*. Maltol, a Maillard reaction product, exerts anti-tumor efficacy in H22 tumor-bearing mice via improving immune function and inducing apoptosis. RSC Advances. 2015; 5: 101850–101859.
[35] Mi X, Hou J, Wang Z, Han Y, Ren S, Hu J, *et al*. The protective effects of maltol on cisplatin-induced nephrotoxicity through the AMPK-mediated PI3K/Akt and p53 signaling pathways. Scientific Reports. 2018; 8: 15922.
[36] Mi X, Hou J, Jiang S, Liu Z, Tang S, Liu X, *et al*. Maltol mitigates thioacetamide-induced liver fibrosis through TGF-β1-mediated activation of PI3K/Akt signaling pathway. Journal of Agricultural and Food Chemistry. 2019; 67: 1392–1401.
[37] Olaniyan OT, Kunle-Alabi OT, Raji Y. Protective effects of methanol extract of Plukenetia conophora seeds and 4H-Pyran-4-One 2,3-Dihydro-3,5-Dihydroxy-6-Methyl on the reproductive function of male Wistar rats treated with cadmium chloride. JBRA Assist Reprod. 2018; 22: 289–300.
[38] Beppu Y, Komura H, Izumo T, Horii Y, Shen J, Tanida M, *et al*. Identificaton of 2,3-dihydro-3,5-dihydroxy-6-methyl-4H-pyran-4-one isolated from Lactobacillus pentosus strain S-PT84 culture supernatants as a compound that stimulates autonomic nerve activities in rats. Journal of Agricultural and Food Chemistry. 2012; 60: 11044–11049.
[39] Ban JO, Hwang IG, Kim TM, Hwang BY, Lee US, Jeong HS, *et al*. Anti-proliferate and pro-apoptotic effects of 2,3-dihydro-3,5-dihydroxy-6-methyl-4H-pyranone through inactivation of NF-kappaB in human colon cancer cells. Archives of Pharmacal Research. 2007; 30: 1455–1463.
[40] Mujeeb F, Bajpai P, Pathak N. Phytochemical evaluation, antimicrobial activity, and determination of bioactive components from leaves of aegle marmelos. BioMed Research International. 2014; 2014: 497606.
[41] The Metabolomics Innovation Centre. Showing metabocard for 5-Hydroxymaltol (HMDB0032988). 2019. Available at: https://hmdb.ca/metabolites/HMDB0032988 (Accessed: 20 June 2020).
[42] Al-Tameme HJ, Hadi MY, Hameed IH. Phytochemical analysis of Urtica dioica leaves by fourier-transform infrared spectroscopy and gas chromatography-mass spectrometry. Journal of Pharmacognosy and Phytotherapy. 2015; 7: 238–252.
[43] Kong F, Lee BH, Wei K. 5-Hydroxymethylfurfural mitigates lipopolysaccharide-stimulated inflammation via suppression of MAPK, NF-kappaB and mTOR activation in RAW 264.7 cells. Molecules. 2019; 24: 275.
[44] Ahn H, Im E, Lee DY, Lee HJ, Jung JH, Kim SH. Antitumor effect of pyrogallol via miR-134 mediated s phase arrest and inhibition of PI3K/AKT/Skp2/cMyc signaling in hepatocellular carcinoma. International Journal of Molecular Sciences. 2019; 20: 3985.
[45] Tamil Selvi S, Jamuna S, Thekan S, Paulsamy S. Profiling of bioactive chemical entities in Barleria buxifolia L. using GC-MS analysis—a significant ethno medicinal plant. Journal of Ayurvedic and Herbal Medicine. 2017; 3: 63–77.
[46] Bordoloi M, Saikia S, Bordoloi PK, Kolita B, Dutta PP, Bhuyan PD, *et al*. Isolation, characterization and antifungal activity of very long chain alkane derivatives from Cinnamomum obtusifolium, Elaeocarpus lanceifolius and Baccaurea sapida. Journal of Molecular Structure. 2017; 1142: 200–210.
[47] Falowo AB, Muchenje V, Hugo A, Aiyegoro OA, Fayemi PO. Antioxidant activities of Moringa oleifera L. and Bidens pilosa L. leaf extracts and their effects on oxidative stability of ground raw beef during refrigeration storage. Journal of Food. 2016; 15: 249–256.
[48] Gok M, Zeybek ND, Bodur E. Butyrylcholinesterase expression is regulated by fatty acids in HepG2 cells. Chemico-Biological Interactions. 2016; 259: 276–281.
[49] National Center for Biotechnology Information. Bioactivity for AID 1082239—SID 194134450. 2020. Available at: https://pubchem.ncbi.nlm.nih.gov/bioassay/1082239#sid=194134450 (Accessed: 20 June 2020).
[50] National Center for Biotechnology Information. Moringa crude extracts and their derived fractions with antifungal activities. 2008. Available at: https://pubchem.ncbi.nlm.nih.gov/patent/US7404975 (Accessed: 20 June 2020).
[51] National Center for Biotechnology Information. Antiandrogenic agent. 2006. Available at: https://pubchem.ncbi.nlm.nih.gov/patent/US7018993 (Accessed: 20 June 2020).
[52] Marzi I, Cowper K, Takei Y, Lindert K, Lemasters JJ, Thurman RG. Methyl palmitate prevents Kupffer cell activation and improves survival after orthotopic liver transplantation in the rat. Transplant International. 1991; 4: 215–220.
[53] El-Demerdash E. Anti-inflammatory and antifibrotic effects of methyl palmitate. Toxicology and Applied Pharmacology. 2011; 254: 238–244.
[54] Saeed NM, El-Demerdash E, Abdel-Rahman HM, Algandaby MM, Al-Abbasi FA, Abdel-Naim AB. Anti-inflammatory activity of methyl palmitate and ethyl palmitate in different experimental rat models. Toxicology and Applied Pharmacology. 2012; 264: 84–93.
[55] Burns TA, Duckett SK, Pratt SL, Jenkins TC. Supplemental palmitoleic (C16:1 cis-9) acid reduces lipogenesis and desaturation in bovine adipocyte cultures. Journal of Animal Science. 2012; 90: 3433–3441.

[56] McGinty D, Letizia CS, Api AM. Fragrance material review on phytol. Food and Chemical Toxicology. 2010; 48 Suppl 3: S59–S63.
[57] Santos CCDMP, Salvadori MS, Mota VG, Costa LM, de Almeida AAC, de Oliveira GAL, *et al*. Antinociceptive and antioxidant activities of phytol *in vivo* and *in vitro* models. Neuroscience Journal. 2013; 2013: 949452.
[58] The Metabolomics Innovation Centre. Showing metabocard for Methyl stearate (HMDB0034154). 2019. Available at: https://hmdb.ca/metabolites/HMDB0034154 (Accessed: 20 June 2020).
[59] The Metabolomics Innovation Centre. Showing metabocard for Arachidic acid (HMDB0002212). 2020. Available at: https://hmdb.ca/metabolites/HMDB0002212 (Accessed: 20 June 2020).
[60] Yang H, Hu G, Chen J, Wang Y, Wang Z. Synthesis, resolution, and antiplatelet activity of 3-substituted 1(3H)-isobenzofuranone. Bioorganic & Medicinal Chemistry Letters. 2007; 17: 5210–5213.
[61] Lozano-Grande MA, Gorinstein S, Espitia-Rangel E, Dávila-Ortiz G, Martínez-Ayala AL. Plant sources, extraction methods, and uses of squalene. International Journal of Agronomy. 2018; 2018: 1829160.
[62] Chen J, Chou E, Duh C, Yang S, Chen I. New cytotoxic tetrahydrofuran- and dihydrofuran-type lignans from the stem of Beilschmiedia tsangii. Planta Medica. 2006; 72: 351–357.
[63] Murugesu S, Ibrahim Z, Ahmed QU, Nik Yusoff NI, Uzir BF, Perumal V, *et al*. Characterization of alpha-glucosidase inhibitors from clinacanthus nutans lindau leaves by gas chromatography-mass spectrometry-based metabolomics and molecular docking simulation. Molecules. 2018; 23: 2402.
[64] Oh MS, Yang JY, Lee HS. Acaricidal toxicity of 2'-hydroxy-4'-methylacetophenone isolated from Angelicae koreana roots and structure-activity relationships of its derivatives. Journal of Agricultural and Food Chemistry. 2012; 60: 3606–3611.
[65] National Center for Biotechnology Information. Insulin receptor partial agonists. 2016. Available at: https://pubchem.ncbi.nlm.nih.gov/patent/US2019177393 (Accessed: 20 June 2020).
[66] Saeedi M, Eslamifar M, Khezri K. Kojic acid applications in cosmetic and pharmaceutical preparations. Biomedicine & Pharmacotherapy. 2019; 110: 582–593.
[67] Du P, Zhang G, Li C, Liu L, Sun L, Liu N, *et al*. Characteristic of microencapsulated 1,3-dioleoyl-2-palmitoylglycerol and its application in infant formula powder. International Journal of Food Properties. 2018; 21: 2355–2365.
[68] Aamir M, Singh VK, Dubey MK, Meena M, Kashyap SP, Katari SK, *et al*. In silico prediction, characterization, molecular docking, and dynamic studies on fungal SDRs as novel targets for searching potential fungicides against fusarium wilt in tomato. Frontiers in Pharmacology. 2018; 9: 1038.
[69] Katiyar C, Gupta A, Kanjilal S, Katiyar S. Drug discovery from plant sources: an integrated approach. Ayu. 2012; 33: 10–19.
[70] Wu S, Tian L. Diverse phytochemicals and bioactivities in the ancient fruit and modern functional food pomegranate (*Punica granatum*). Molecules. 2017; 22: 1606.
[71] Barathikannan K, Venkatadri B, Khusro A, Al-Dhabi NA, Agastian P, Arasu MV, *et al*. Chemical analysis of Punica granatum fruit peel and its *in vitro* and *in vivo* biological properties. BMC Complementary and Alternative Medicine. 2016; 16: 264.
[72] Bekir J, Mars M, Souchard JP, Bouajila J. Assessment of antioxidant, anti-inflammatory, anti-cholinesterase and cytotoxic activities of pomegranate (Punica granatum) leaves. Food and Chemical Toxicology. 2013; 55: 470–475.
[73] Daina A, Michielin O, Zoete V. SwissADME. A free web tool to evaluate pharmacokinetics, drug-likeness and medicinal chemistry friendliness of small molecules. Scientific Reports. 2017; 7: 42717.
[74] Davies MR, Wang K, Mirams GR, Caruso A, Noble D, Walz A, *et al*. Recent developments in using mechanistic cardiac modelling for drug safety evaluation. Drug Discovery Today. 2018; 21: 924–938.
[75] Hase T, Tanaka H, Suzuki Y, Nakagawa S, Kitano H. Structure of protein interaction networks and their implications on drug design. PLoS Computational Biology. 2009; 5: e1000550.
[76] Safari-Alighiarloo N, Taghizadeh M, Rezaei-Tavirani M, Goliaei B, Peyvandi AA. Protein-protein interaction networks (PPI) and complex diseases. Gastroenterology and Hepatology from Bed to Bench. 2014; 7: 17–31.
[77] Ramsay RR, Popovic-Nikolic MR, Nikolic K, Uliassi E, Bolognesi ML. A perspective on multi-target drug discovery and design for complex diseases. Clinical and Translational Medicine. 2018; 7: 3.
[78] Paterni I, Granchi C, Katzenellenbogen JA, Minutolo F. Estrogen receptors alpha (ERalpha) and beta (ERbeta): subtype-selective ligands and clinical potential. Steroids. 2014; 90: 13–29.
[79] Yugandhar P, Kumar KK, Neeraja P, Savithramma N. Isolation, characterization and in silico docking studies of synergistic estrogen receptor a anticancer polyphenols from Syzygium alternifolium (Wt.) Walp. Journal of Intercultural Ethnopharmacology. 2017; 6: 296–310.

Keywords: Breast cancer; Docking; MD simulations; GC-MS/MS profiling; Natural compounds; Pomegranate; Estrogen receptor; ADMET; 4-coumaric acid methyl ester

Send correspondence to: Sushil Kumar Middha, DBT-BIF Facility, Department of Biotechnology, Maharani Lakshmi Ammanni College for Women, 560012 Bangalore, India, E-mail: drsushilmiddha@gmail.com